Electrocatalytic CO<inf>2</inf> conversion to C<inf>2</inf> products: Catalysts design, market perspectives and techno-economic aspects

Renewable and Sustainable Energy Reviews 161 (2022) 112329

Contents lists available at ScienceDirect

Renewable and Sustainable Energy Reviews

journal homepage: www.elsevier.com/locate/rser

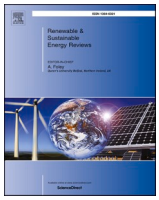

Electrocatalytic CO_2 conversion to C_2 products: Catalysts design, market perspectives and techno-economic aspects

Estela Ruiz-López [a,**], Jesús Gandara-Loe [a], Francisco Baena-Moreno [b,c], Tomas Ramirez Reina [a,d,*], José Antonio Odriozola [a,d]

[a] Department of Inorganic Chemistry and Material Sciences Institute of Seville, University of Seville-CSIC, 41092, Seville, Spain
[b] Department of Space, Earth and Environment, Chalmers University of Technology, Göteborg, 412 96, Sweden
[c] Chemical and Environmental Engineering Department, Technical School of Engineering, University of Seville, C/ Camino de Los Descubrimientos S/n, Sevilla, 41092, Spain
[d] Department of Chemical and Process Engineering, University of Surrey, GU2 7XH, Guildford, United Kingdom

ARTICLE INFO

Keywords:
CO_2 reduction
Electrocatalysts
C_2 products
Electrochemical reduction
Techno-economic analysis

ABSTRACT

The energy crisis caused by the incessant growth in global energy demand joint to its associated greenhouse emissions motivates the urgent need to control and mitigate atmospheric CO_2 levels. Leveraging CO_2 as carbon pool to produce value-added products represents a cornerstone of the circular economy. Among the CO_2 utilization strategies, electrochemical reduction of CO_2 conversion to produce fuels and chemicals is booming due to its versatility and end-product flexibility. Herein most of the studies focused on C_1 products although C_2 and C_{2+} compounds are chemically and economically more appealing targets requiring advanced catalytic materials. Still, despite the complex pathways for C_{2+} products formation, their multiple and assorted applications have motivated the search of suitable electrocatalysts. In this review, we gather and analyse in a comprehensive manner the progress made regarding C_{2+} products considering not only the catalyst design and the electrochemistry features but also techno-economic aspects in order to envisage the most profitable scenarios. This state-of-the-art analysis showcases that electrochemical reduction of CO_2 to C_2 products will play a key role in the decarbonisation of the chemical industry paving the way towards a low-carbon future.

1. Introduction

The constant growth in global energy demand has entailed a massive consumption and excessive depletion of fossil fuels, leading to an energy crisis as well as a health crisis due to greenhouse gas emissions, responsible for climate change and global temperature increase. The atmospheric CO_2 level (one of the main greenhouse gases contributors) has also increased, reaching a value of 416.47 ppm (May 2020) [1] and is forecast to reach up to 570 ppm by 2100 [2], while the safety limit is estimated at 350 ppm [3]. As a result, there is an urgent need to control and mitigate these emissions by pursuing low-carbon alternatives including CO_2 capture, sequestration, and utilization [1]. Indeed, research efforts are focused on the use of CO_2 as carbon pool, given its potential to become genuine feedstock to produce value-added products hence turning a problem into a virtue.

Nonetheless, conversion of CO_2 is an arduous task given its high thermodynamic stability due to the two strong equivalent C═O linear bonds; bonds that possess a much higher bonding energy (750 kJ mol^{-1}) than that of other carbon bonds (C–H, 411 kJ mol^{-1}; C–C, 336 kJ mol^{-1}; C–O, 327 kJ mol^{-1}) [4]. Therefore, a suitable CO_2 transformation route must overcome these energy barriers requiring high energy input, preferably coming from carbon-neutral sources, as well as the use of an active catalyst or high pressures and temperatures [5–7]. Among all the possible techniques to convert CO_2, including thermochemical, electrochemical, photochemical and biological processes [1,7–9], electrochemical reduction of CO_2 has attained a growing interest due to its multiple possible uses in the energy sector and chemical industries, producing value-added fuels and chemicals at mild conditions and in a carbon-neutral way [10–12].

Electrochemical reduction of CO_2 allows tuning the selectivity of the value-added products obtained [13]. Traditionally, research on electrocatalytic reduction of CO_2 has mainly focused on the formation of C_1

* Corresponding author. Department of Inorganic Chemistry and Material Sciences Institute of Seville, University of Seville-CSIC, 41092, Seville, Spain.
** Corresponding author.
E-mail addresses: eruizl@us.es (E. Ruiz-López), t.ramirezreina@surrey.ac.uk (T.R. Reina).

https://doi.org/10.1016/j.rser.2022.112329
Received 27 May 2021; Received in revised form 14 January 2022; Accepted 25 February 2022
Available online 9 March 2022

products (such as CO, formate and methanol) since these simple $2e^-$ transfer reactions are kinetically more favourable [14,15]. However, the production of C_{2+} species would be rather interesting from the application perspective [16]. C_{2+} alcohols contain higher energy densities, lower toxicity and corrosiveness compared to methanol, being more suitable as blending or even pure fuels in existing internal combustion engines; and short-chain alkanes can be directly injected into gas-distribution grids enhancing the calorific value of natural gas or biogas. They can also be regarded as entry platform chemicals for current value chains, e.g. light olefins for the production of polymers [9,17]. Moreover, and taking acetate as an example, its direct production from the electrochemical reduction of CO_2 is a more efficient and effective process in terms of energy and steps compared to the traditional industrial multistep process from fossil fuels, besides more environmentally friendly from a CO_2 emissions point of view [14].

However, C_{2+} products reaction pathways are complex and strongly influenced by the catalyst surface, electrode materials, reaction medium (buffer strength and electrolyte solution), design of electrochemical cell or working conditions such as temperature, pH or pressure and concentration of CO_2 [18,19]. The high C–C coupling activation energy required joint to its bond formation competition with C–H and C–O bond formations limit the efficiency towards C_{2+} products. The later along with the overpotential gap between the essential CO intermediates formation and that of C_{2+} species are the main impediments in the practical application of CO_2 reduction to C_{2+} species in commercial electrolysers. Indeed, these aspects are regarded as the major bottlenecks accounting for the low energy efficiency of C_{2+} products compared to C_1 counterparts [19,20]. Still the commercial appetite and their extraordinary added value makes necessary to strengthen the research efforts towards direct CO_2 to C_{2+} products.

In order to achieve the practical viability and implementation of this technology, higher efficiency and energy requirements as well as lower operational costs must be met. Electricity plays a key role in the profitability of the CO_2 reduction reaction (CO_2RR), being the main factor in the operational costs [21,22]. Nonetheless, one of the advantages of the electrochemical reduction of CO_2 is that it can be approached as an efficient way to store all excess electrical green energy (generated from unpredictable and intermittent sources such as wind and solar) as transportable chemicals and fuels [23]. Regarding the efficiency requirements, commercial electrolysers require current densities above 200 mA cm^{-2} as well as long-term durability catalysts [21,24,25]. For these reasons, research on the development of efficient catalysts is encouraged.

Recently, several efforts have been made to obtain suitable electrocatalysts, able to improve catalytic activity and selectivity by controlling their chemical states, size, morphology, surface defects, crystal facets, porosity or by creating heterostructures [6,20,26–28]. Generally, catalysts explored for the electrochemical reduction of CO_2 are based on metals. While formic acid is the main product using Sn, Pb, In, Hg or Bi as catalysts; Zn, Ag, Au and Pd have been found to be selective towards CO [10,23,29]. In the case of C_{2+} products, Cu has demonstrated a unique ability to facilitate C–C coupling, although it is not a selective catalyst since numerous C_1–C_3 hydrocarbon and oxygenate products have been observed on Cu surface [19,30].

In this scenario and given the research gaps and motivation for this appealing CO_2 conversion route, herein we analyse the recent advances and efforts in the electrochemical CO_2 reduction to C_{2+} products. Beyond summarising the fundamental aspects for the development of a suitable catalyst as well as the mechanistic pathways of the most industrially desired C_{2+} species, this review makes emphasis on key aspects to design highly selective electrocatalysts. Additionally, as a very important aspect not frequently addressed in electrocatalysis literature, we bring techno-economical requirements into discussion targeting potential industrial implementation.

2. Fundamental aspects of electrochemical CO_2 conversion

Electrocatalytic CO_2 reduction is especially appealing due to the wide variety of important products derived from it and their multiple advantages. The process can be carried out in neutral pH, at room temperature and atmospheric pressure and it can be controlled by the reaction temperature and the electrode potential. The chemical consumption can be minimised since electrolytes can be completely recycled and the intermittent renewable energy can be converted into stable chemical energy. Moreover, the system is modular, compact and easy to scale-up [8,9,13,31]. However, despite all the advantages, some drawbacks must be overcome for the technology to fully take off at commercial level. The activation of the very stable CO_2 molecule is the first step in its electrochemical reduction and requires high overpotential. In fact, the formation via single-electron transfer of CO_2*- radical intermediate (E = −1.9 V vs. SHE) is considered as the rate-determining step on most transition metal-based catalysts [3,32]. In general, heterogeneous electrocatalytic reactions take place at the catalyst surface-electrolyte interface [33], so the main CO_2 electroreduction process could be simplified as follows: CO_2 chemisorption and bond forming interaction on the catalyst surface, electron and/or proton transfers leading to C–H, C–O bonds or C–C coupling; and product species rearrangement and desorption from the catalyst surface into the electrolyte [3,20,34], While formate and CO generation from C–O and C–H has been further studied and can be achieved upon implementing the right electrocatalyst at low overpotential [32], hydrocarbon or alcohol production is a more complex task. A summary of the most accepted activation routes for the electrochemical CO_2 reduction to C_{2+} products is given in Fig. 1 [12,19,20,32].

Due to the multiple reaction pathways that can be conducted in parallel and competitive ways as well as more complex pathways that are not elucidated yet, a wide-ranging product distribution is generally obtained. The reaction pathways and, consequently, product distributions strongly depend on the electrocatalyst. Noble metals (Ag, Au and Pd) have been found as high selective catalysts for C1 products like CO and formic acid, while activity towards more than 2e− products such as methanol and methane has been obtained with Cu-based catalysts [12]. Besides the choice of a selective electrocatalyst, product distribution can be also adjusted by tuning external parameters such as the electrode characteristics (surface, morphology, facets, …), operation conditions (applied overpotential, electrolyte, anodic reaction) or the cell design itself.

2.1. Electrolyte

In general, electrolytes should provide stable pH at bulk, good ionic conductivity and moderate to high CO_2 solubility [22]. The type, concentration and composition of electrolytes have been found to affect CO_2 electrochemical reduction. One of the most common and favourable electrolytes is alkaline aqueous solution because it stands lower overpotential than its neutral counterpart [22,35], helps to supress the hydrogen evolution reaction (Eq. (1)) and provides a high conductivity which reduces ohmic losses [35]. Hydrogen evolution reaction (HER) (equation (1)) is the main competing reaction to CO_2 reduction. Due to the proton insufficiency on the catalyst surface, a basic media helps to supress this undesired reaction boosting CO_2 electrochemical reduction products [35,36].

$$2H^+ + 2e^- \rightarrow H_2 \quad (1)$$

In the study of Verma et al. [37] it was observed with different alkaline aqueous solutions higher current densities as increasing the solutions concentrations and through electrochemical impedance spectroscopies demonstrated the decrease of the cell resistance due to the ionic conductivity increase while increased the concentrations. Moreover, as Gabardo et al. reported [35], a 240-mV positive shift of the onset potential was achieved while using a 10 M KOH solution as electrolyte

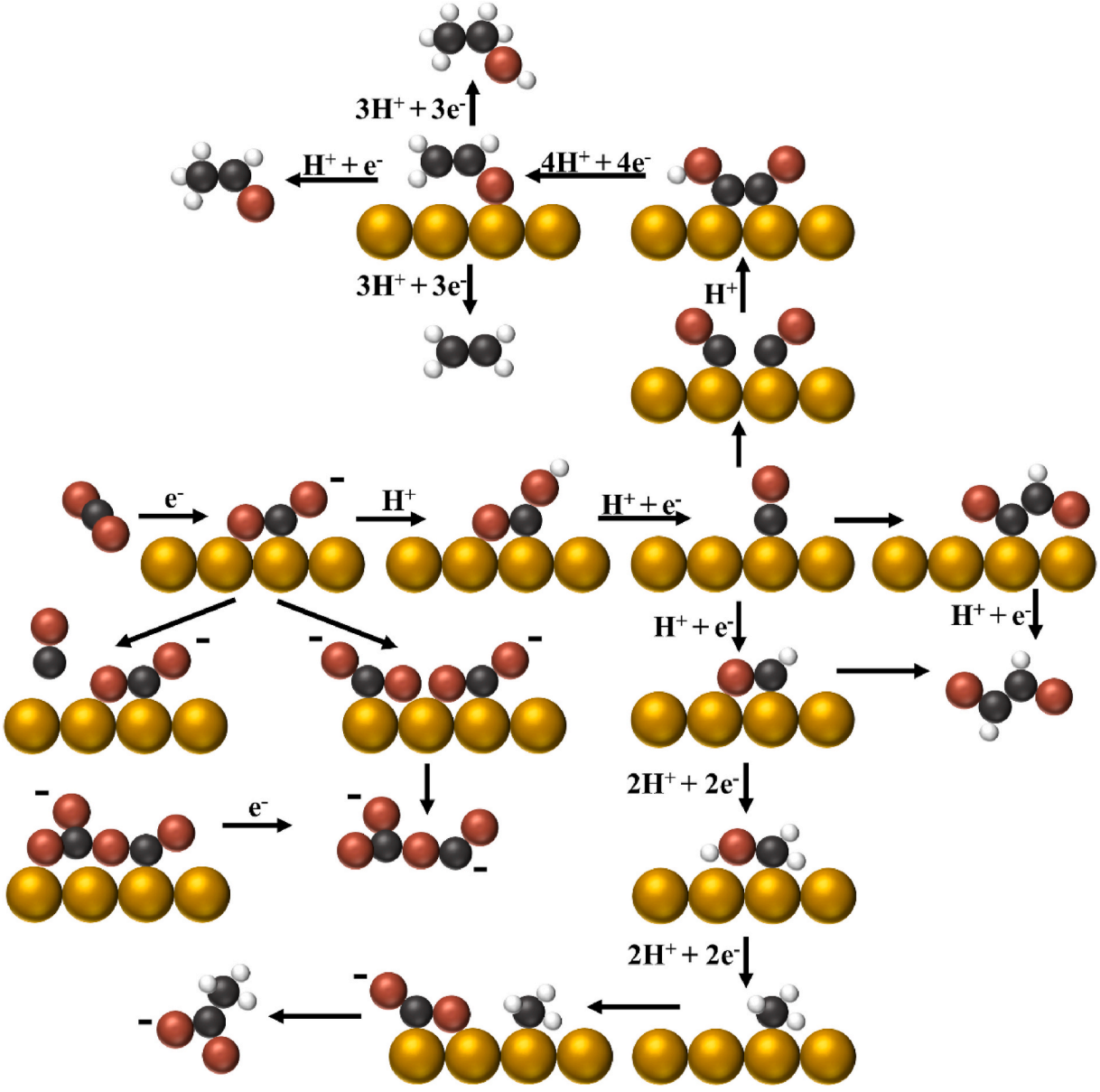

Fig. 1. Electrochemical CO_2 reduction reaction pathways to C_2 products [12,19,20,32].

instead of a 1 M KOH one.

The CO_2 solubility can be increased using organic solvents instead of water solutions as electrolytes. Although CO_2 is a nonpolar molecule, it possesses an appreciable polarizability and an ability to accept hydrogen bonds from suitable donor solvent [38]. Most of the organic electrolytes are polar solvents and allow the electrochemical CO_2 reduction in a wider potential window [20]. The use of an aprotic solvent (such as acetonitrile or dimethylformamide) enables the *CO–CO dimerization while CH_4 production is favoured in a protic solvent. Nonetheless, electrochemical CO_2 reduction can be tuned by adding protic compounds to aprotic solvents in order to facilitate the generation of H-containing products [20]. Some research on the use of ionic liquids (added to aqueous or organic solvents) has been made looking for a higher conductivity and hence, a decrease in overpotential [39–41]. Ionic liquids (ILs) could be proper electrolytes since they have good thermal stability, high CO_2 solubility, wide electrochemical window, low vapor pressure and partially HER inhibition [20,42]. However, ILs also present some drawbacks concerning their high cost, the environmental toxicity embedded in their production, liquid products extraction struggling [43] or cathodic corrosion [44]. The latest works where ILs has been used as electrolyte are summarised in Table 1. Cathodic catalysts can suffer from deactivation due to the presence of trace impurities (metal ions or organics) coming not only from noble metal anodic catalysts dissolved because of operating conditions [45], but from the electrolyte, being the main deactivation cause in Cu, Ag and Au catalysts [46]. However, deactivation due to impurities can be avoided if a pre-electrolysis with a sacrificial electrode or an irreversible coordination between metal ions and a chelating agent (e.g. ethylenediaminetetraacetic acid) are conducted [46].

2.1.1. pH

As depicted in Fig. 1, the formation of C_{2+} products through different reaction pathways depends on the protonation process. The protonation transfer can affect the product distribution in electrochemical CO_2 reduction, therefore, pH near the catalyst electrode surface, bulk pH, and local pH were found to affect the final product distribution [6].

Due to the consumption of protons near the electrode surface as a result of proton and water reduction, a local pH (usually more alkaline

Table 1
Latest works where an ionic liquid has been used as electrolyte for CO_2RR.

IL	Electrolyte	Catalyst	Major product	FE (%)	Potential	Current density ($mA{\cdot}cm^{-2}$)	Ref.
$[BMIM]BF_4$	$[BMIM]BF_4$:H_2O 1:3	Atomically dispersed Sn catalysts on defective CuO	Methanol	88.6	−2.0 V vs. Ag/Ag^+	67	[47]
	$[BMIM]BF_4$:CH_3CN:H_2O 30:65:5 (wt %)	Mn–N_3(SAC) embedded in g-C_3N_4	CO	>90	0.62 V (overpotential)	29.7	[48]
	$[BMIM]BF_4$:CH_3CN:H_2O 30:65:5 (wt %)	I treated porous N-doped carbon	CO	~100	−2.2 V vs. Ag/Ag^+	38.2	[49]
	0.1 M $[BMIM]BF_4$/PC	Ag	CO	98.5	−1.9 V vs. Fc/Fc^+	8.2	[50]
	$[BMIM]BF_4$ aqueous solution	Pd–Cu bimetallic aerogel	Methanol	80	−2.1 V vs. Ag/Ag^+	31.8	[51]
[BMIM]Otf	100 mM $TBAPF_6$ and 100 mM [BMIM] Otf in CH_3CN	Bi-based CO	CO	90	−2.05 V vs. SCE	20	[52]
$[BMIM]PF_6$	$[BMIM]PF_6$:CH_3CN:H_2O 30:65:5 (wt %)	Porous ZnO nanosheets with OH group	CO	97.8	−2.0 V vs. Ag/Ag^+	44.3	[53]
	0.5 M $[BMIM]PF_6$ in CH_3CN	Atomic In anchored on N-doped carbon	CO	97.2	−2.1 V vs. Ag/Ag^+	39.4	[54]
	0.1 M $[BMIM]PF_6$ and 0.1 M $TEAPF_6$ in CH_3CN	CoPc-DrGO	CO	93.1	−2.6 V vs. Ag/Ag^+	122	[55]
$[Bu_4N]BF_4$	0.1 M $[Bu_4N]BF_4$/PC	Ag	CO	85	−1.9 V vs. Fc/Fc^+	2.7	[50]
$[BZMIM]BF_4$	$[BZMIM]BF_4$: CH_3CN:H_2O 14.7:73.6:11.7 (wt%)	PbO_2	Formic acid	95.5	−2.3 V vs. Ag/Ag^+	40.8	[56]
$[EMIM]BF_4$	$[EMIM]BF_4$:$NaHCO_3$ 90:10 (%v/v)	Nanoporous Au films	CO	96.6	−0.55 V vs. RHE	4.5	[57]
	$[EMIM]BF_4$:H_2O 92:8 (%v/v)	3D Ag nanoflower coated Al foam	CO	75	−1.8 V vs. Pt	36.6	[58]
[EMIM][OTf]	[EMIM][OTf]:CH_3CN:H_2O 81:14:5 (wt%)	PbSn alloy sheets	Formate	91	−1.95 V vs. Ag/AgCl	7.7	[59]
$TBAPF_6$	100 mM $TBAPF_6$ and 100 mM [BMIM] Otf in CH_3CN	Bi-based CO	CO	90	−2.05 V vs. SCE	20	[52]
$TEAPF_6$	0.1 M $[BMIM]PF_6$ and 0.1 M $TEAPF_6$ in CH_3CN	CoPc-DrGO	CO	93.1	−2.6 V vs. Ag/Ag^+	122	[55]
[TEA][4-MF-PhO]	0.9 M [TEA][4-MF-PhO] in CH_3CN	Pb	Oxalic acid	86	−2.6 V vs. Ag/Ag^+	9.03	[60]

than bulk pH) can be generated [32]. This difference in pH is caused by mass transport limitations [61] and depends on the operation conditions: current density, bulk pH, types of cations or anions, and on the electrode morphology [6,32,61]. Providing the adequate electrolyte with the right pH is a key factor to control the reaction pathway and the stability of the reaction intermediates [19,62]. As an example, it has been reported that selectivity towards ethylene on Cu electrocatalysts can be fine-tuned by modifying the buffering capacity. At high local pH, ethylene production through *CO–CO dimerization pathway is both kinetically and thermodynamically favourable, whereas the C_1 pathway is suppressed [63,64].

2.1.2. Ions effect

In accordance with pH effect, H^+ and OH^- concentration has been shown to influence both, the activity and selectivity of the electrochemical CO_2 reduction. Comparing several electrolytes containing potassium precursors (KCl, K_2SO_4, $KClO_4$), phosphate buffer and $KHCO_3$ aqueous solution diluted and concentrated, it was found that diluted $KHCO_3$ KCl, K_2SO_4, $KClO_4$ solutions favoured the formation of C_2H_4 and alcohols [65,66]. The presence of OH^- anions produced from electrochemical reactions provokes a pH increase in the electrocatalyst surface enhancing C_2 selectivity by suppressing HER [63,67]. Concentrated electrolytes (concentrated $KHCO_3$ and phosphate buffer) are capable of neutralising this OH^- anions. The local pH does not differ from the bulk pH and CH_4 formation is favoured [65].

Besides H^+ and OH^- ions, the electrolyte cations and anions nature was also reported to have a significant effect on product selectivity. Increasing size of alkali cation from Li^+ to Cs^+ usually leads to higher electrochemical CO_2 reduction rates and higher C_2/C_1 products. This behaviour was attributed to differences in the local pH and changes in the electrochemical potential in the outer Helmholtz plane (OHP) due to the cation size [68]. The presence of hydrated alkali metal cations located at the edge of the Helmholtz plane stabilises the adsorption of surface intermediates such as $*CO_2$, which is the intermediate precursor to the formation of C_2 products through C–C coupling. Slighter cations are strongly hydrated, hindering cation-specific adsorption on the electrode surface [12]. Larger cations are more energetically favoured at the OHP than smaller ones, hence an increase in cation size typically leads to a large cations coverage [68].

The influence of halide anions on electrochemical CO_2 reduction has also been studied. The halide adsorption on the catalyst surface affects to the activity, selectivity, and the electronic structure, depending on the halide size and its concentration [69,70]. It has been reported that adsorbed halide anions could limit the proton adsorption, inhibiting HER [71]. While using Cu as electrocatalyst, halides are able to stabilize the *CO intermediate through the formation of a covalent Cu-halide interaction [69]. Due to this increase in *CO population on the catalyst surface, adding Cl^-, Br^- and I^- to the electrolyte can lead to an increase in CO selectivity and hence a large methane production [69], or a lower overpotential and an increase in CO_2 reduction rate while keeping C_2–C_3 faradaic efficiencies [70]. Among the mentioned halides, KI electrolyte led to the highest *CO formation on the catalyst surface and then, the highest C_2 selectivity [72].

2.2. Pressure and temperature effects

Working at higher pressures encompasses the possibility of operating at higher temperatures and an increase in the CO_2 solubility according to Henry's law [73]. This increase favours the adsorption of CO_2 species on the catalyst surface due to the higher CO_2 concentration in the electrolyte [22], and some works have reported higher current densities by increasing CO_2 partial pressure [73,74]. Therefore, changing the CO_2 partial pressure can tune the relative surface coverage and hence, the stability of CO_2 reduction intermediates and the product selectivity [35]. The combination of both, an increase in the reaction pressure and a highly alkaline environment could improve CO selectivity and energy efficiency reaching industry relevant current density values [35]. Nevertheless, working at high pressures imposes some drawbacks since an unbalanced pressure could result in drying the catalyst surface or flooding of the catholyte causing operational issues [22].

Regarding the temperature effect, it has rarely been studied and most studies were conducted at ambient temperature. An increase of

temperature implies a lower CO_2 solubility, so the undesired HER will prevail over the CO_2 reduction process. Moreover, the temperature increase is also limited by the possible membrane degradation, the operational window is rather narrow, although it could be widened if coupled with a pressurised system [22]. In general, higher temperatures lead to higher currents since ionic conductivity increases and the diffusion coefficient also rises, thus the CO_2 transport is more efficient [75]. The CO_2 solubility problem could be overcome while supplying CO_2 and water vapor in a gas phase electrolyser provided with a proper gas diffusion electrode (GDE). That way, the reaction kinetics would be enhanced due to the higher temperature and would compensate the poor solubility [22,75]. Nonetheless, further studies of temperature effects should be conducted in order to achieve the optimal operation conditions and assess its economic viability.

The effects of pressure and temperature strongly depend on the cell design, i.e., their permissible and adequate values are certainly disparate if a gas phase system or a liquid phase system is used, and additional studies are needed. However, and considering the limited available studies, it could be stated that slightly higher than ambient conditions of pressure and temperature would be favourable in terms of product selectivity and reaction rate [22].

2.3. Overpotential

The energy barrier between the onset potential and the standard reduction potential, the overpotential, is highly dependent on the working electrode. The different ranges of the applied overpotential can affect the preferable pathways to form C–C coupling. The *CO–COH coupling is dominant at high overpotentials, while the *CO–CO dimerization is favoured at low overpotentials [6,19].

2.4. Anodic reaction

Up-to-date, CO_2 cathodic reaction has usually been coupled with anodic water oxidation since water electrolysis is a well-known process without mass transport limitations, and all accomplishments and knowledge achieved in water electrolysers can be adapted to CO_2 electrolysers [76]. However, oxygen evolution reaction (OER) requires a high overpotential that limits the energy efficiency of the whole electrolyser (OER can consume up to 90% electricity in CO_2RR [77]) and oxygen gas could corrode and oxidise metallic catalysts or cell components [22]. Replacing this reaction for another with lower cell voltage requirements and providing high-value anodic products while maintaining a free of emissions process could be of interest. The work of Vass et al. [76] reviews and summarises different interesting alternatives to the widely used OER, including the CO_2RR coupled with an already existing technology, the use of industrial waste as sacrificial agents or the production of raw and fine chemicals [78–80]. In the case of Li et al. [77], possible anodic oxidation reactions have been summarised and classified attending to the desired cathodic and/or anodic products. Some of the valued-added anode processes that have been lately paired up with CO_2RR are summarised in Table 2. Moreover, first technoeconomic analysis have shown promising results concerning CO_2RR coupled with organic compounds oxidation [81], achieving an electricity consumption save up to 53% in the case of the glycerol oxidation [78]. Notwithstanding, the complexity of coupling CO_2 cathodic reaction with these anodic reactions in terms of operation conditions, cell design and structure, product separation is still a challenge that requires further research (see Table 3).

2.5. Cell design

Significant efforts and improvements have been made on developing a suitable electrocatalytic reaction system that enhances the electrochemical CO_2 reduction reaction [13,22,25]. As represented in Fig. 2, electrochemical reaction systems can be categorised into H-cell systems, flow cell systems and microfluidic reactors.

H-type cells are widely used because of their simple assembly, operation and products separation, their versatile configurations and low cost. In this system, working and reference electrodes are fixed in the cathodic reaction chamber while counter reaction is fixed in the anodic one. Both chambers are prefilled with the electrolyte and work without recycling. Their main disadvantage is the low CO_2 solubility in the liquid electrolyte, which limits the current density [98], as well as the large distance between electrodes [99]. Moreover, selectivity towards C_{2+} products has always been diminished in favour of HER [13]. For all mentioned above, H-type cells are a suitable batch reactor for studying and comparing different electrocatalysts and products in lab-scale, although they do not fit in further industrial applications.

The main component of the flow cell systems is the membrane-

Table 2
Latest value-added anodic processes paired up with CO_2RR.

Anodic reaction	Equation	Electrolyte	Anodic catalyst	Anodic main product	Ref.
Methanol oxidation	$CH_3OH + H_2O \rightarrow CO_2 + 6H^+ + 6e^-$	0.5 M KOH	$Pd/MnFe_2O_4$ NSs	CO_2	[82]
	$CH_3OH + 4OH^- \rightarrow HCOOH + 3H_2O + 4e^-$	1 M KOH	Ni-MOF NSs	HCOOH	[83]
		1 M KOH	$Ni(OH)_2$/Ni foam	HCOOH	[84]
		1 M KOH	CuONS/CF	HCOOH	[85]
		1 M KOH	NiCo-MOF	HCOOH	[86]
Ethanol oxidation	$CH_3CH_2OH + H_2O \rightarrow CH_3COOH + 4H^+ + 4e^-$	0.5 M $NaHCO_3$	Pt mesh – TEMPO	Acetic acid	[87]
	$CH_3CH_2OH + OH^- \rightarrow CH_3COO^- + 2H_2$	4 M KOH	Nanostructured Pd@Ti	Acetate	[88]
Isopropanol oxidation	$C_3H_8O \rightarrow C_3H_6O + 2H^+ + 2e^-$	0.5 M $NaHCO_3$	Pt mesh – TEMPO	Acetone	[87]
1,2-propanediol oxidation	$C_3H_8O_2 + H_2O \rightarrow C_3H_6O_3 + 4H^+ + 4e^-$	0.5 M $KHCO_3$/0.5 M K_2CO_3	ACT-TEMPO	Lactic acid	[89]
Glycerol oxidation	$C_3H_8O_3 + 2OH^- \rightarrow C_3H_6O_3 + 2H_2O + 2e^-$	0.5 M HCO_3^-/CO_3^{2-}	STEMPO	Glyceraldehyde	[90]
	$C_3H_8O_3 + 8OH^- \rightarrow 3HCOOH + 5H_2O + 8e^-$	2 M KOH	$CoSe_2$/CC	Formic acid	[91]
Benzyl alcohol oxidation	$PhCH_2OH \rightarrow PhCHO + 2H^+ + 2e^-$	0.5 M acetate/0.5 M Na_2SO_4	Nano-ITO	Benzaldehyde	[92]
1-phenylethanol oxidation	$C_8H_{10}O \rightarrow C_8H_8O + 2H^+ + 2e^-$	0.5 M $NaHCO_3$	Pt mesh – TEMPO	Acetophenone	[87]
4-methoxybenzyl alcohol oxidation	$C_8H_{10}O_2 \rightarrow C_8H_8O_2 + 2H^+ + 2e^-$	0.5 M $NaHCO_3$	Pt mesh – TEMPO	4-methoxybenzaldehyde	[87]
Ammonia oxidation	$2NH_3 \rightarrow N_2 + 6H^+ + 6e^-$	5 M KOH	Pt	N_2	[80]
Urea oxidation	$(NH_2)_2CO + H_2O \rightarrow CO_2 + N_2 + 6H^+ + 6e^-$	5 M KOH	Ni	N_2, CO_2	[80]
HMF oxidation	$HMF + 4OH^- \rightarrow FFCA + 4H_2O + 4e^-$; $HMF + 6OH^- \rightarrow FDCA + 6H_2O + 6e^-$	0.5 M $KHCO_3$	NiO NPs	FFCA, FDCA	[93]
NaCl oxidation	$Cl^- + 2OH^- \rightarrow ClO^- + H_2O + 2e^-$	0.5 M NaCl	RuO_2/Ti	ClO^-	[94]
SO_3^{2-} oxidation	$SO_3^{2-} + 2OH^- \rightarrow SO_4^{2-} + H_2O + 2e^-$	0.3 M Na_2SO_4	IrO_2–Ta_2O_5/Ti	SO_4^{2-}	[95]
Chlor-alkali reaction	$2Cl^- \rightarrow Cl_2 + 2e^-$	1 M HCl	Ru-based DSA	Cl_2	[96]
		KCl saturated	DSA	Cl_2	[79]
Organic pollutants removal	*p*-nitrophenol oxidation	0.5 M KCl	Ti/SnO_2–Sb	–	[97]

Table 3
Most important characteristics and findings of the techno-economic analysis available in the literature.

Ref.	Aim of the study	C_2 product targeted	Economic parameter evaluated	Main findings
[244]	Identifying potential CO_2 reduction profitable products	Ethylene Ethanol	Price to reach profitable scenarios	Key performance targets are Faradaic Efficiency (90%), Cell Voltage (<1.8 V), Current Density (>300 mA cm^{-2}), and Stability (>80 000 h).
[24]	Evaluate the techno-economic feasibility of producing different C_1–C_2 chemicals	Ethylene Ethanol	Gross margin (difference between revenues and costs divided revenues)	Carbon monoxide and formic acid are the most economically viable products. Ethanol and ethylene could reach profitability if co-produced with the two previously mentioned.
[243]	Economic evaluation of 100 ton/day plant for various CO_2 reduced products	Propanol Ethanol Ethylene	Net present value	To reach profitability, improvement in performances is needed: 300 mA cm^{-2} and 0.5 V overpotential at 70% Faradaic efficiency.
[251]	Reduce CO_2 losses to crossover and carbonate formation, trough analysing the costs of different alternatives	Ethylene	Cost analysis	Current lab scale scenario: 5800–7800 $/ton Optimistic scenario: 1200–3800 $/ton
[119]	Review different alternatives for CO_2 utilization, giving some estimations for electrocatalytic CO_2 reduced products.	Propanol Ethanol Ethylene	Levelized cost per ton of product from CO_2 reduction	Assuming very optimistic scenario (electrolyser cost of $500/kW, energy conversion efficiency of 60%, Faradaic efficiency of 90%, electricity cost of 2 ¢/kWh, and CO_2 cost of 30$/ton), ethylene, propanol and ethanol can be competitive with current prices.

electrode assembly (MEA), where the electrodes are assembled to the solid polymer electrolyte or membrane, which acts a separation barrier of the chambers and is in charge of ion transportation between them. Depending on the type of ion transported, membranes can be cation exchange membrane (CEM), i.e., protons are transported from the anolyte to the cathodic chamber; anion exchange membrane (AEM), where hydroxide ions are transported from the anode to the cathode or the combination of both, bipolar membrane (BPM).

According to the way of feeding the CO_2 into the cell, two cell systems can be distinguished: gas phase and liquid phase electrolyser. In the former type, a humidified gaseous CO_2 stream can be directly used as feedstock at cathode, enhancing this way mass diffusion and production rates [13]. The use of this cell design has also been reported to increase CO selectivity [100], to improve partial current density and stability for formate production [101], and to selectively generate C_{2+} products [14,102].

In the liquid phase electrolysers, liquid electrolyte is in both electrodes. For that reason, the system can be pressurised and CO_2 can be fed without further humidification [35]. In general, these flow cells have shown a better electrochemical CO_2 reduction performance compared with H-type cells, mainly due to the enhanced CO_2 diffusion and the local gas-electrolyte-catalyst interface [13].

Microfluidic cells are an attractive alternative electrolyser configuration where, in some cases, the membrane is replaced by a thin gap between the electrodes filled with flowing electrolyte stream. The CO_2 molecules are easily diffused into the electrode-electrolyte interface. Besides avoiding issues related to membrane degradation and cost, its absence allows wider pH and reaction temperature windows [103]. However, the existence of crossover could result in the products oxidation at some extent, although a multichannel design, a nanoporous separator [104] or a dual-electrolyte system [105] could solve this problem.

2.6. Electrode surface and morphology

The electrode surface and morphology has been reported to strongly affect in the activity and selectivity on the electrochemical CO_2 reduction. Formation of defect sites, nano or complex structures, subsurface oxygen or crystal facets (schemed in Fig. 3) are the dependant factors [13,32].

2.6.1. Defect sites

The formation of defect sites from vacancies or grain boundaries has been pointed out as the responsible of increasing activity and selectivity in electrochemical CO_2 reduction [106,107]. Grain boundaries can alter the surfer properties of particles, generating active sites and inducing a large surface catalytic area [26]. These modifications of the particles and the catalyst surface can lead to a lower energy barrier for CO_2 reduction or to an enhancement of CO adsorption and the C–C bond formation with a consequent stabilization of C_2 intermediates and higher selectivity for this C_{2+} products [107,108].

2.6.2. Structure

Several efforts have been made to create nanostructured catalysts more active and selective than bulk or foil electrocatalysts. It was found that roughened Cu electrodes could provide a high local pH, which promotes C_2H_4 generation over CH_4 [109,110]. Catalyst structure is capable of controlling C_{2+} products selectivity by tuning the pore size and depth of nanostructures such as nanowire arrays, nanofoams, nanoparticles or nanocubes [111–113]. Smaller and deeper pores increase ion concentration and intermediates residence times, enhancing C_{2+} products selectivity. Moreover, intermediates can be confined into the nanostructure generating long chain molecules [26,114].

2.6.3. Facets

Besides physical factors, the intrinsic catalyst properties could also affect the activity and selectivity [19] and several studies have proved the strong facet dependence on electrochemical CO_2 reduction product selectivity [6,19]. As an example, it has been observed in Cu catalysts that Cu(100) favours selectivity towards ethylene and the C–C coupling improving C_{2+} products selectivity while Cu(111) favours the methane and formate formation [67,115,116].

2.6.4. Oxidation states

The electrocatalyst performance could also be adjusted by tuning the oxidation states via oxide-derived materials. Using again the copper catalysts as an example, it was observed that Cu oxidation states can easily change during electrochemical reaction conditions and oxide-derived catalysts enhance the activity and selectivity towards C_{2+}

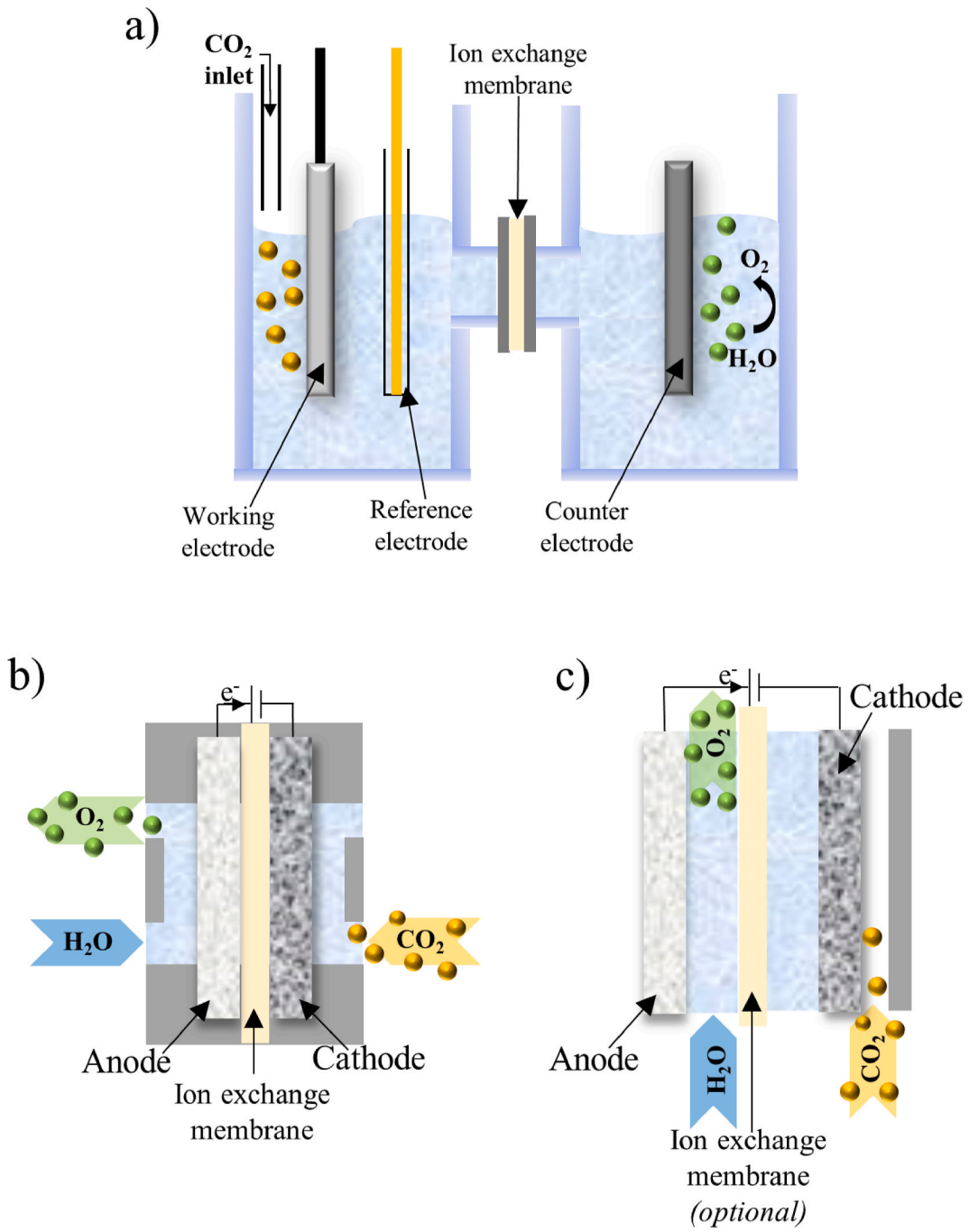

Fig. 2. Electrochemical reaction systems: a) H-cell, b) flow cell, c) microfluidic cell.

products [6,19]. The presence of residual oxygen, subsurface oxygen or oxidized cooper states favours the stabilization of the intermediates thus enhancing C–C coupling [117,118].

3. Product distribution based on electrocatalyst design

As mentioned before, due to the multiple possible reaction pathways, numerous products can be originated. However, product distribution can be tuned by designing an active and selective electrocatalyst. The complex formation of C_{2+} products is gaining attention due to their higher energy density and economic value [119], and several research projects are currently focused on their production [120–122]. The numerous and assorted applications, where these products can be valuable, are summarised in Fig. 4. The search of a catalyst with adequate electronic properties to be selective for the C–C coupling is vital to generate species with one or more C–C bonds. Among metals, copper has been found particularly active for the formation of C_{2+} compounds, although a few non copper-based catalysts such as heteroatom-doped carbon materials [123], NiP [124], NiGa [125] or PdAu [126] have shown significant formation of C_{2+} species. In the following subsections we will discuss the catalysts design to successfully facilitate the production of key C_2 and C_{2+} products which are highly appealing for the chemical industry and whose electrochemical production might result in a game-changing approach.

3.1. CO_2 to oxalate/acetate

3.1.1. Oxalate. Oxalate or oxalic acid is the simplest dicarboxylic

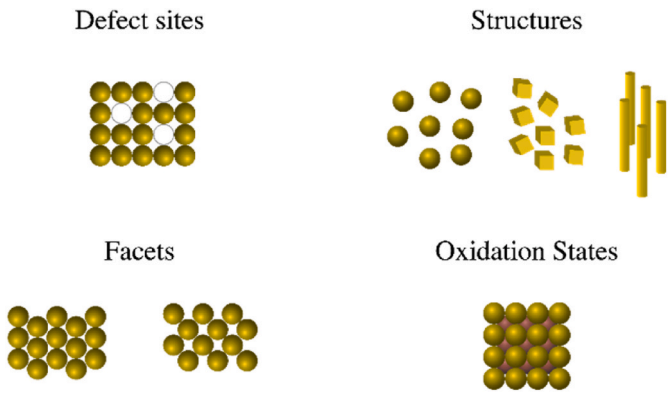

Fig. 3. Electrode surface and morphology factors that affect to the electrochemical performance.

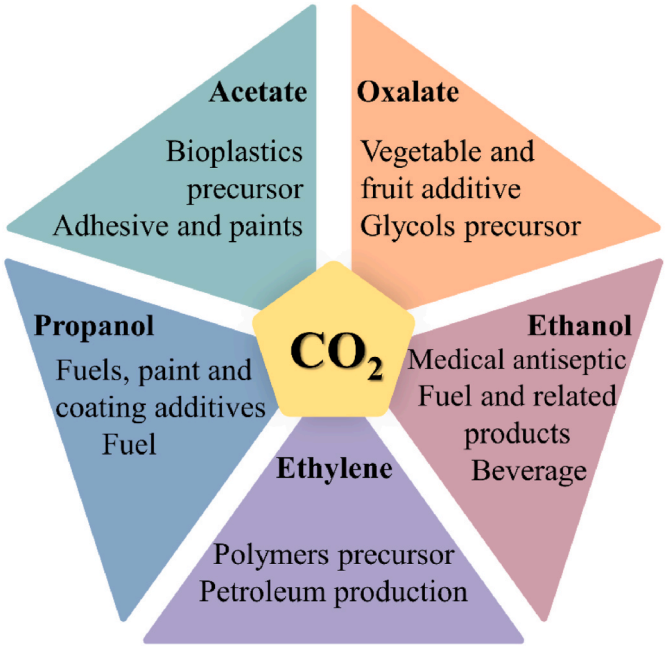

Fig. 4. Main applications of C_{2+} products.

acid widely used in the chemical industry in applications such as pharmaceuticals and textiles manufacturing, rare earth extraction, oil refining or metal processing [127–130]. Oxalate is a precursor to glycols, which are in turn precursors to valuable synthetic materials [131,132]. Some research has been done concerning the beneficial effect of its application to improve quality of some vegetable and fruits and to extend their storage time and prevent its early degradation [133–135] and its role in the recovery of valuable metal ions from lithium-ion batteries [136,137]. Regarding current investigations, oxalic acid effect is being subject of study in a treatment to a honeybee's disease [138].

The electrochemical CO_2 reduction products strongly depend on both the chemical nature of the electrode and the reaction medium. In a protic solvent as water, formate would be the main product [139,140]. Since the solubility of CO_2 in aqueous solutions is really low (about 30 mM), water molecules would be available nearby the electrode surface and HER would be favoured. In fact, only hydrogen is yielded while water is the only component of the electrolyte, the charge transfer proceeds favourable to water [141]. Using aprotic solutions that provide a higher solubility (about 240 mM in acetonitrile as an example [141]) as solvents would lead to CO_2^{*-} intermediate disproportionation to carbon monoxide and carbonate or dimerization to oxalate ions [139]. Besides their higher CO_2 solubility, aprotic nonaqueous solvents such as acetonitrile, dimethyl formamide, dimethyl sulfoxide or propylene carbonate have been widely used because of their large cathodic window and the inhibition of HER [130,142].

In this aprotic medium, CO and carbonate were reported as the major products using metals such as Pt, Pd, In, Zn, Sn or Au as catalysts, while oxalic has been reported as the major product using a Pb, Sn or Hg electrode [143,144].

It is known that the first and primary step on the electrochemical CO_2 reduction is the formation of the intermediate radical ion CO_2^{*-}, a change and mass-transfer controlled reaction that must be conducted at a sufficiently cathodically polarized electrode. In a nonaqueous aprotic medium, two main competitive pathways have been repeatedly described in literature: nucleophilic coupling of CO_2^{*-} with nearby CO_2, that could produce CO and carbonate, or oxalate through ECE mechanism; and the purely dimerization of two radical ions following an EC mechanism, which would also lead to an oxalate anion production [131,140,141,143,145–147]. Dimerization reaction is more favourable at high concentrations of CO_2^{*-} radical anions while the reductive disproportionation of CO_2 could be conducted at low CO_2^{*-} concentrations [148]. The reaction mechanism for oxalate production is depicted in Fig. 5.

Lead has traditionally been chosen as the working cathode due to its high HER overpotential and its low cost, which favours CO_2 reduction [143,144,147,149]. In nonaqueous medium, oxalate has been reported as the main product and oxalate faradaic efficiencies (FEs) exceeding 80% were registered from the very early studies [143,144]. The work of Eneau-Innocent et al. studied the role of Pb electrode in a propylene carbonate electrolyte [142]. Propylene carbonate large electrochemical window, CO_2 solubility and relative low toxicity made this aprotic solvent suitable for the electrochemical reduction. It was found that Pb electrodes are very selective towards oxalate via direct dimerization route. In situ IR spectroscopy measurements revealed that unstable intermediate CO_2^{*-} radical ions evolve quickly to adsorbed Pb–CO_2^{*-}, which dimerizes, and oxalate is finally desorbed.

Some studies have also explored Pb or stainless steel electrodes coupled with sacrificial anodic electrodes in order to easily remove oxalate product from the electrochemical system [130,147,148]. Zinc has been widely used as a sacrificial anode because it produces zinc cation which fast reacts with oxalate anion towards insoluble zinc oxalate, preventing the further reduction or oxidation reaction of oxalate anion [147]. Lv et al. achieved a 96.8% FE for producing oxalate in 0.1 M tetrabutylammonium perchlorate in acetonitrile with a lead cathode and a zinc sacrificial anode [147]. Such a high efficiency was a result of a combination of two factors: water total elimination and low temperature

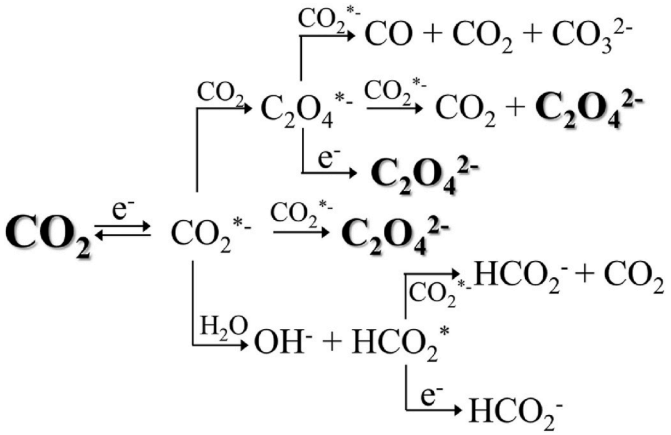

Fig. 5. Electrochemical CO_2 reduction reaction pathways to oxalate generation [139,140,145].

(5 °C), as shown in Fig. 6. As observed in the reaction mechanism (Fig. 5), the presence of water in the electrochemical CO_2 reduction negatively affects to oxalate selectivity (see Fig. 6) [60]. Therefore, in this study [147], the electrochemical system was subjected to a pre-electrolysis and CO_2 desiccation process in order to remove possible trace of water from the electrolyte and from CO_2. It was found a decrease up to 40% in oxalate FE where 1.25 v/v% of water was added to the electrolyte solution, confirming the interferences of water in electrochemical CO_2 reduction. In the case of temperature effect, solubility of CO_2 increases while decreasing the temperature, enhancing CO_2 availability on the electrode surface for its reduction.

The advantages of incorporating ILs as electrolytes were also explored for oxalate production in Pb electrodes. A novel aromatic ester anion functionalized IL of 4-(methoxycarbonyl) phenol tetraethylammonium ([TEA][4-MF-PhO]) was designed based on catalytic and

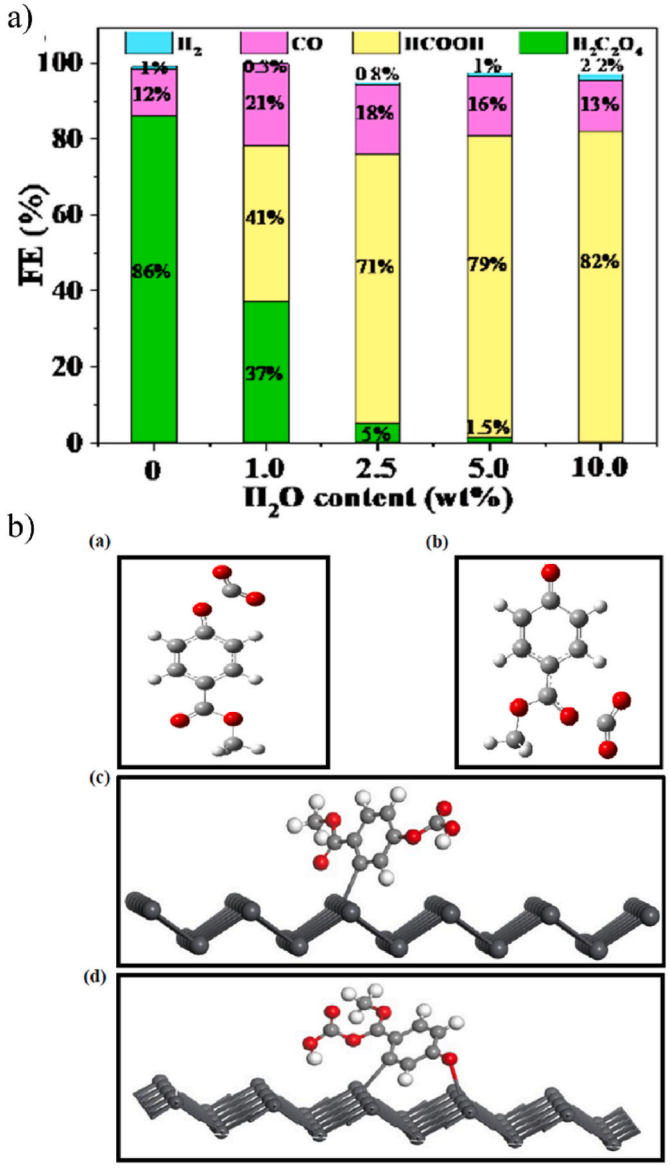

Fig. 6. a) The effect of H_2O on the faradaic efficiency of CO_2 reduction products in the IL electrolyte at −2.6 V (Vs. Ag/Ag^+); b) The function of IL anion of [4-MF-PhO]- on CO_2 capture, activation, and transformation. Interaction between CO_2 and aromatic ester anion with (a) phenolic and (b) ester groups. (c) and (d) The activation and reaction of CO_2 at the Pb electrode surface with the aid of $[4\text{-MF-PhO}]^-$ and H^+. Reprinted with permission from Ref. 60. Copyright © 2020 Wiley-VCH GmbH.

stability properties of aromatic esters and quaternary ammonium salts, respectively [60]. DFT calculations were performed in order to investigate the interaction between aromatic ester anion of $[4\text{-MF-PhO}]^-$ and CO_2 revealing the ability of the anion with phenoxy and ester double active sites to bend the stable CO_2 molecule to CO_2^{*-}. H^+ cations provided by anolyte were combined with the anion-radical generating $[4\text{-MF-PhO-COOH}]^-$ that eventually dimerized to oxalic acid (Fig. 6). High partial current densities (9.03 mA cm^{-2}) and acceptable FEs (86%) obtained on Pb electrode in [TEA][4-MF-PhO]-acetonitrile electrolyte assert the integration of IL in this aprotic electroreduction systems for oxalate production and open a potential path of research and improvement.

Besides all progress related to Pb or stainless steel electrodes, cathodic materials such as metal organic frameworks (MOFs), metal-complexes or carbon supported metals have also been explored to perform the electrochemical CO_2 reduction to oxalate [132,150–152]. Metal organic frameworks are porous materials with a crystalline ordered structure capable of storing CO_2, which have also presented attractive features such as high porosity or thermal stability and adjustable chemical functionality [153–155]. They are indeed an emerging family showing promising features for electro and thermal catalysis [156] and their careful implementation in CO_2 to oxalate process merits further studies.

Shentil Kumar et al. coated Cu-BTC on a glassy carbon electrode to prove it as an efficient electrocatalyst for the oxalate production from CO_2 [151]. The electrochemically synthesized MOF was capable of sequestrating and electro reducing CO_2 simultaneously. The electrochemical reduction can be conducted inside the pores through heterogeneous electron transfer between the MOFs and the previously adsorbed and compressed CO_2 molecules, generating a 90% pure oxalic acid with a FE of 51%.

Silver was also tested as cathodic catalyst in a carbon-silver hybrid configuration [150]. Babassu coconut, an important Brazilian vegetation that has been previously used for nanocarbon production [157], has been hydrothermally carbonised in the presence of silver nitrate solution, obtaining the Ag@C catalytic system (see Fig. 7). Comparing the results obtained with this system with those in absence of silver nanoparticles, it can be concluded that silver nanoparticles enabled the charge transfer for the CO_2 reduction besides enhancing the electrocatalytic activity. Moreover, synthesis with longer residence times resulted in larger deposits of silver particles that influenced the size of the carbon spheres and increased oxalic acid production.

As opposed to the previous works, Paris et al. reported the use of a Cr–Ga electrode supported on glassy carbon to produce oxalate in a KCl aqueous solution electrolyte [158]. This catalytic system consisted of a Cr_2O_3–Ga_2O_3 thin alloy film and, whereas neither Cr_2O_3 nor Ga_2O_3 films alone could produce oxalate, the alloy of the two oxides led to oxalate FE of 59% at a pH of 4.1. Organic solvent or those with low proton availability reported the production of the oxalate dianion; however, in this aqueous system, a combination of monoanionic and dianionic species was generated. The Cr–Ga system originates a more appealing product distribution since protonated oxalates are more desired species from an industrial point of view [158].

Oxalate was obtained at a more positive potential than that required for CO_2^{*-} intermediate generation, i.e., this process provides a CO_2^{*-} independent and lower energetic pathway than those previously reported (Fig. 5). This low energetic reaction pathway could involve a C_1 product as oxalate precursor, and experiments feeding CO, formate, methanol or their combinations instead of CO_2 were conducted. It was observed that CO-methanol combination did lead to oxalate production. Labelling experiments showed that carbon atoms oxalated derived from CO, although both methanol and CO are required for its production. Results obtained from this report encourage additional studies to advance in oxalate production in aqueous solutions [158].

3.1.2. Acetate. As already mentioned, the traditional synthesis of acetic acid involves a three-step energy-intensive process (methane or

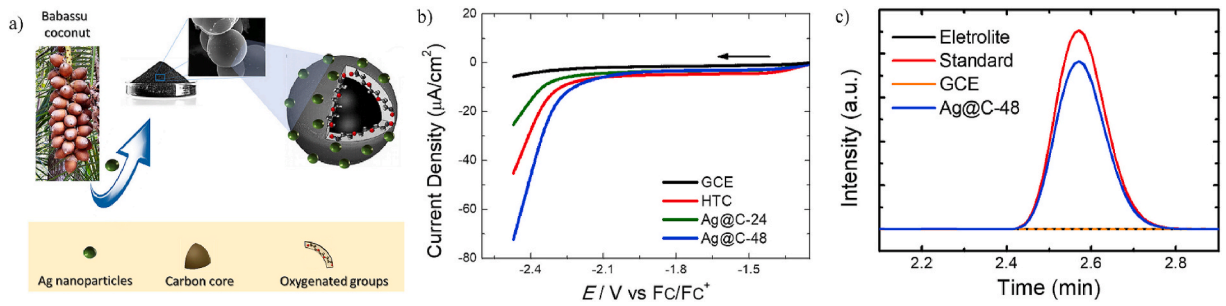

Fig. 7. a) Configuration of the Ag@C system, b) linear sweep voltammetry measurements of bare GCE and the different synthesized catalysts supported on GCE in 0.1 mol L^{-1} TBA-HFP/acetonitrile solution at a scan rate of 10 mV s^{-1} (cathodic direction), c) standard commercial oxalic acid (10 μg/mL in a 0.1 mol L^{-1} solution of tetra-*n*-butylammonium hexafluorophosphate in acetonitrile) (red) and its comparison with the chromatogram after 3 h of chronoamperometry with the Ag@C-48-modified GCE (blue). Reprinted with permission from Ref. 150. Copyright © 2020 Elsevier Ltd.

coal to syngas, syngas to methanol and methanol carbonylation to acetic acid) using methane or coal as feedstocks [159,160]. Therefore, an efficient direct production of acetic acid can revolutionise the production of this key chemical. Indeed, acetate is not only an important end-product, but a versatile platform chemical capable of producing medium-chain fatty acids, alcohols and bioplastics, e.g., vinyl acetate monomers, esters and acetic anhydride [161,162]. Further, some industrial processes like denitrification or biological phosphorus removal also use acetate as carbon substrate [163].

Unfortunately, acetate has not received a lot of attention as product of electrochemical CO_2 reduction. The reaction pathway for its formation remains certainly unclear, although several possible routes have been suggested (as depicted in Fig. 8). At high potentials and high local pH, ethanol and acetate could be directly produced from acetaldehyde via Cannizzaro-type reaction [164]. Garza et al. pointed out that the ratio ethanol/acetate did not follow the proposed reaction [165]. They suggested the existence of additional pathways, such as the acetate production as a by-product on the ethylene pathway through $*OCH_2$-COH dimerization to a three-membered ring compound and further reduction.

In general, the formation of CO_2^{*-} radical anion was accepted as the first step in the electrochemical CO_2 reduction [16,123]. Genovese et al. provided experimental evidence for the acetic acid formation from a nucleophilic attack of $*CH_3$ adsorbed species by this intermediate radical anion [16]. Once the radical anion was adsorbed, it can be reduced at the electrode surface until a $–CH_2OH$ specie is originated, and then generating methanol or proceeding with reduction until $–CH_3$ species generation. In the case of conducting the electrochemical reduction on a N-doped nanodiamond/Si rod array electrocatalysts, the in situ infrared spectroscopy identified OOC-COO as intermediate [123]. Based on the assumption that kinetics C–C coupling is faster than CO_2^{*-} protonation [166], the pathway proposed involves the combination of two radical anions to generate the OOC-COO intermediate that would be further protonated and reduced producing acetate. Following the same assumption and while using Cu(I)/C- doped boron nitride as catalyst in the presence of 1-ethyl-3-methylimidazolium tetrafluoroborate ([Emim]BF4)–LiI solution, Sun et al. proposed the formation of a $[Emim–CO_2]^+$ complex that reduces the electron transfer barrier to CO adsorption [160]. CO adsorbed is then reduced and protonated until methanol formation (detected product) that would couple with CO_2^{*-} to generate acetate. This process is promoted by the presence of the Lewis acidic cation Li^+ and the strong nucleophilicity of I^-, although a more detailed mechanism involving these species needs further investigation.

Alternatives to the above describe route has also been proposed ruling out CO_2^{*-} generation. This is the case of the works of Panglipur et al. [89] and Grace et al. [167] In the former one, acetic acid is

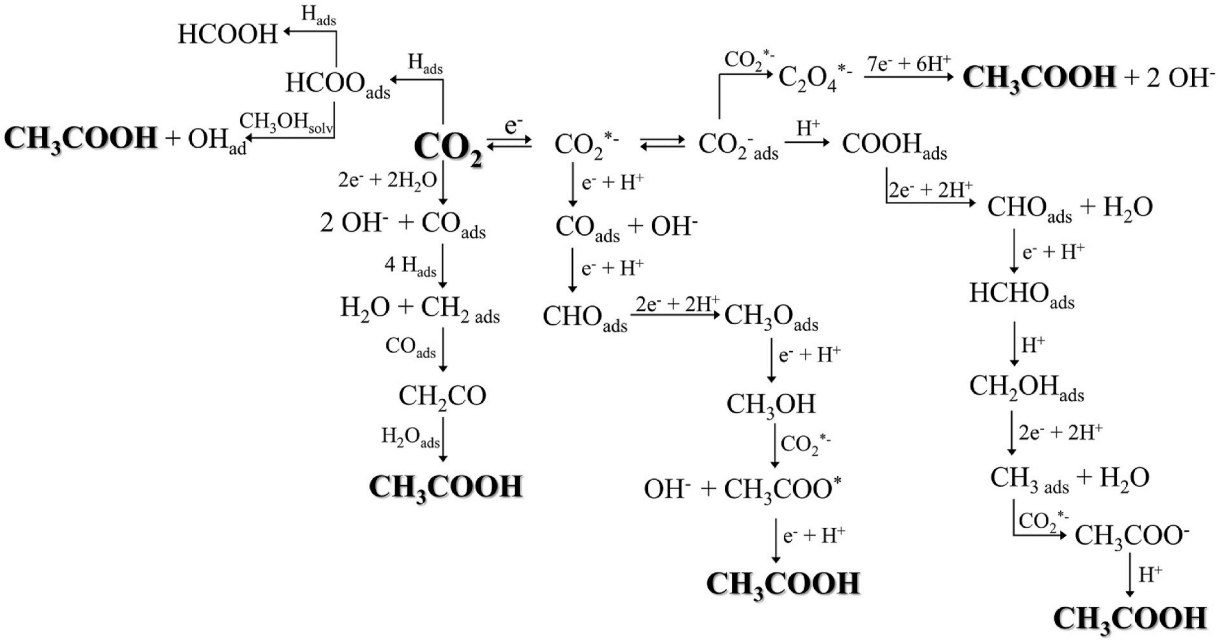

Fig. 8. Electrochemical CO_2 reduction reaction pathways to acetate production [16,89,123,167].

believed to be generated by the formation and adsorption of CO and H^+ species, which would generate CH_2 that, in turn, could react with CO and be hydrated until acetic acid generation [89]. In the second work, due to the ANH groups of polyaniline catalyst and the use of methanol as electrolyte, H adatoms are generated on the electrode surface and then transferred to the CO_2 molecules generating formic acid that could be attacked by the methanol and form acetic acid [167].

Although copper-based catalysts are the most suitable for C_{2+} products from CO_2, bulk copper catalysts face limitations (poor selectivity, high energy input, low activity) that must be overcome tuning these copper catalysts. More selective catalysts can be generated with smaller nanoparticles, defect sites, core-shell structures, oxidation states or heteroatomic doping [168]. In that sense, several tuned copper-based catalysts have reported high faradaic efficiencies toward acetic acid or acetate.

The choice of a suitable support could be a key to improve bulk copper performance. The incorporation of conducting polymers such as polyaniline have been proved to decrease the electrochemical CO_2 reduction overpotential [167]. Cu_2O nanoparticles, with oxygen species to easily adsorb CO_2 and Cu^+ ions promoting CO_2 reduction as active sites, were disposed in a polyaniline matrix. This configuration led to a synergistic effect which allows the generation of acetic acid as the main product with an efficiency of 63% [167].

Boron-doped diamond (BDD) has been widely used in electrochemical application due to its adequate characteristics for those purposes [169]. Although it is able to produce formaldehyde on its own under ambient conditions [89], as support of copper particles, it resulted in a selective electrode to acetic acid generation. Acetic acid was not observed while using copper or BDD as electrodes separately [89]. Same behaviour was observed in an electrocatalyst based on copper nanoparticles supported on carbon nanotubes (CNTs), achieving a production of acetic acid with a selectivity close to 60% [16].

Pure titanium oxide does not present activity in the electrochemical CO_2 reduction process itself [170], but its ability to control the local pH and its good conductivity make nanotubular TiO_2 array (TNA) a suitable support. In the work of Zang et al. TNA was applied as the support of a modified polyoxometalate Cu catalyst [168]. Polyoxometalates (a type of transition metal oxygen anion clusters) were induced to modify the local electronic and protonic environment of Cu nanoparticles conforming a Mo_8 modified cubic fragmented Cu submicron particles on TNA (Mo_8@Cu/TNA) catalytic system. The skeleton structure and SEM images of the catalytic system can be observed in Fig. 9.

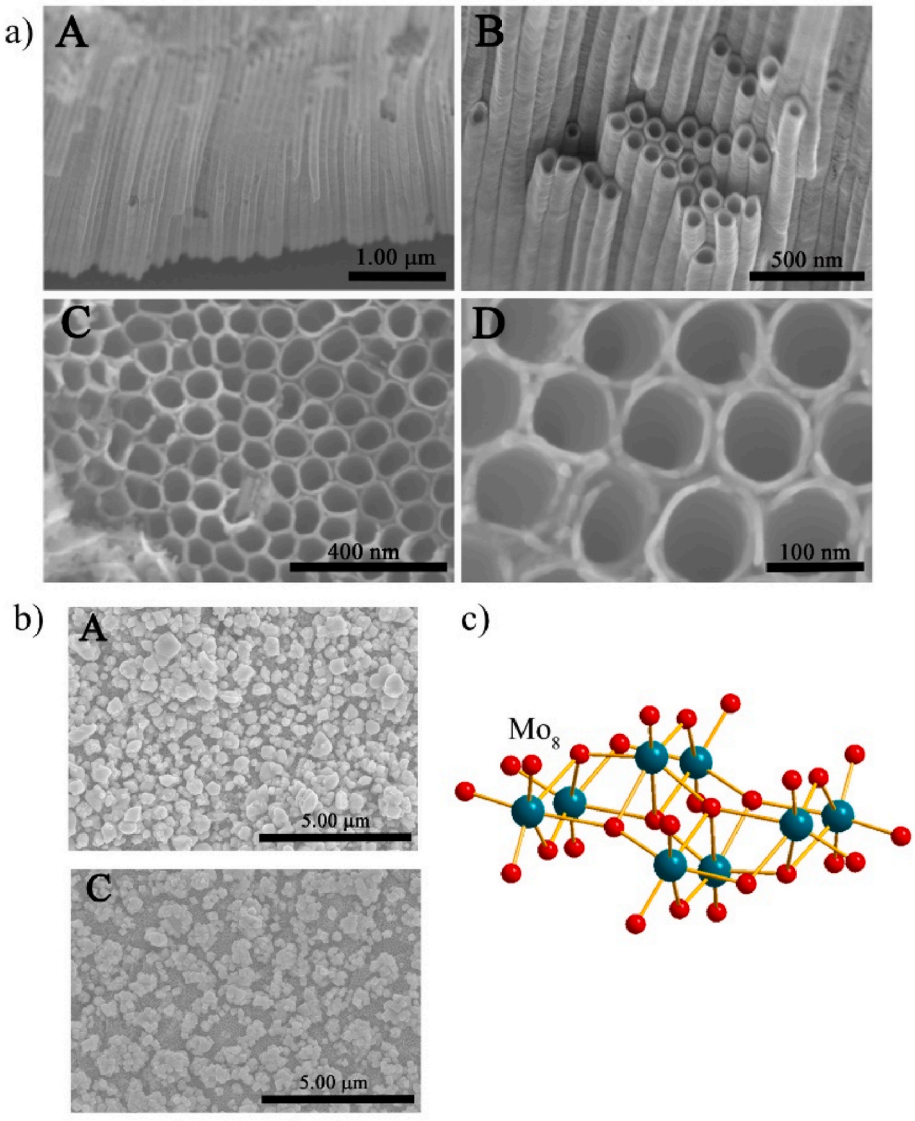

Fig. 9. a) SEM of TiO_2 nano tube array (TNTA); A, B: side views; C, D: top views. b) SEM of the obtained Cu/TNTA, (A) Cu/TNTA, C) Mo_8@Cu/TNA. c) Polyanion skeleton structure of Mo_8. Reprinted with permission from Ref. 168. Copyright © 2020 Elsevier B·V.

Acetate is originated following the single carbon coupling pathway (schemed in Fig. 8), i.e., CO_2 molecules were coupled with formed $*CH_3$. Experiments on mechanism investigation showed the synergistic effects of Cu planes and polyoxometalate cluster promoting the generation of the intermediate $*CH_3$ tuning the selectivity towards acetate. Moreover, Mo oxide clusters modified Cu catalyst obtaining a fragmented Cu surface rich on grain boundaries. Ag was selected as metal to substitute Cu, but in view of selectivity and FE obtained while using Ag instead of Cu, these control experiments just served to highlight the synergistic effect between Cu surface and Mo oxides.

Wang et al. also incorporated Ag in the electrocatalyst, but combined with Cu, forming clusters (~ 6 nm) of Cu and Ag on the surfaces of electropolymerized films, (Cu)m, (Ag)n/polymer/GCE [171]. The increase in the acetate formation as Ag was added to the nanoparticles evidenced the important role of surface metal composition. As observed in Fig. 10, it is believed that the presence of Ag could modified reaction mechanism although is still uncertain. Ag catalysts are able to promote CO_2 reduction to CO [172], so Ag sites could facilitate the CO formation that would be further captured on neighbouring Cu sites for C–C bond formation and later acetate production (Fig. 10).

N-doped systems also represent an appealing family of materials for electrochemical CO_2 conversion. Indeed, they are chemically and active stable compounds that present an overpotential for HER higher than most reported electrocatalysts [173]. This way electrochemical CO_2 reduction could be conducted suppressing H_2O reduction and hence, enhancing the selectivity for the desired product [174]. Boron nitride (BN) promotes the CO_2 chemisorption in the presence of electrons, thus the role of a C-doped BN as support of a Cu(I) complex Cu(I)/BN-C for acetic acid production was evaluated achieving a FE of 80.3% [160]. The support and the catalyst complex behaviours were evaluated separately, finding that bulk BN is not active for CO_2 reduction, but BN-C can generate large amounts of formic acid since N-doped carbon materials can absorb CO_2 and stabilize CO_2^{*-} [175]. The high selectivity to acetic acid is then related to a synergistic effect between catalyst complex and BN-C. CO_2 is first adsorbed and converted into CO_2^{*-} due to BN-C and then protonated and reduced into methanol that would generate the desired acetic acid via C–C coupling with the help of the Cu metal center [160].

Due to the observed proper characteristics of N-doped materials, N-doped nanodiamond supported on a Si rod array (NDD/Si RA) (schemed in Fig. 11) was tested for electrochemical CO_2 reduction showing high efficiency, fast kinetics and good selectivity towards acetate [123]. As observed in Fig. 11, an increase in the N content led to an enhance in acetate and formate production rates due to the defects sites presence and the carbon atoms polarized by the N doping [176]. Defects sites and polarized carbon atoms may promote CO_2 adsorption and CO_2*- stabilization and rod array structure provides a large surface area that facilitates electron transfer. The combination of all these effects would explain the promising results obtained [123].

As mentioned before, Cu-based catalysts have shown excellent performance on electrochemical CO_2 reduction and high selectivity towards C_{2+} products, although they are not the only ones and, as in the case of the N-doped nanodiamond catalyst, modified Fe, Mn, Au, Pd or In metals have demonstrated its activity and selectivity towards acetic acid [15, 177–180].

Fe oxyhydroxide nanostructures (Ferihydrite-like clusters, Fh-FeOOH) were also supported on N-doped graphitic materials (Fe/N–C), and FE values were up to 97% with a high selectivity to acetic acid [177]. Results supporting the same clusters on O-doped carbon were not so encouraging, revealing the favourable Fe–N interaction. N-dopants allowed the stabilization of Fe(II) species instead of Fe_0 (as in the case of using O-dopants) that promotes HER. Acetic acid formation was attributed to the presence of these Fe(II) species adjacent to N sites, while Fe(II) species are believed to reduce HCO_3^- species, N sites enable the C–C coupling.

Indium metal favours the formation of C_1 products, although modifying its electronic properties inducing transitions metal oxygen anion clusters such as polyoxometalate (which has also reported beneficial effects modifying Cu electrodes) [168] can tune its selectivity towards C_{2+} products. Li et al. [180] and Zha et al. [15] works have incorporated polyoxometalates as electrolyte to assist In for the electrochemical CO_2 reduction. As expected, the electrocatalytic performance of In resulted in the formation of hydrogen and formic acid as the only products. The addition of $SiW_{11}Mn$ to the electrolyte gave a result the appearance of acetic acid as well as hydrogen and formic acid, according to ion chromatography, gas chromatography and mass spectrometry analyses [180]. The presence of $SiW_{11}Mn$ reduced the overpotential and enriched In_0 species since it enabled the re-reduction of elemental In.

In the case of adding SiW_9V_3 to the electrolyte, the reaction mechanism was investigated through IR monitoring experiments and gas chromatography [15]. Control experiments (electrolyte without adding SiW_9V_3, and SiW_9V_3 electrolyte without In metal as catalyst) reported

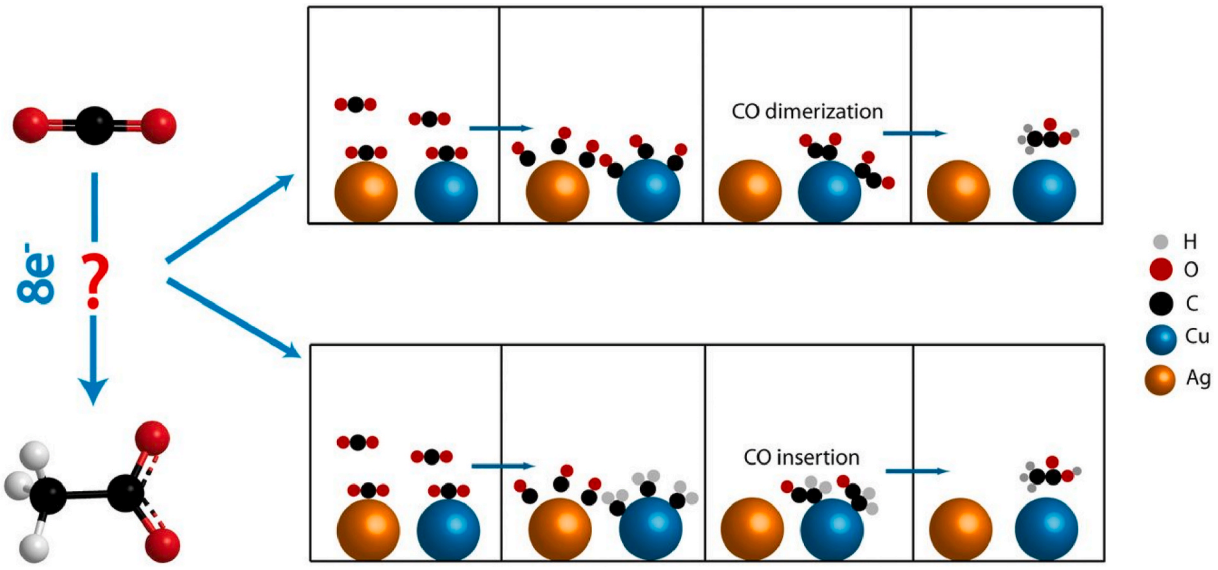

Fig. 10. Possible reaction mechanism for CO_2 reduction to acetate on $(Cu)_m$, $(Ag)_n$/polymer/GCE electrodes. Reprinted with permission from Ref. 171. Copyright © 2018 National Academy of Sciences.

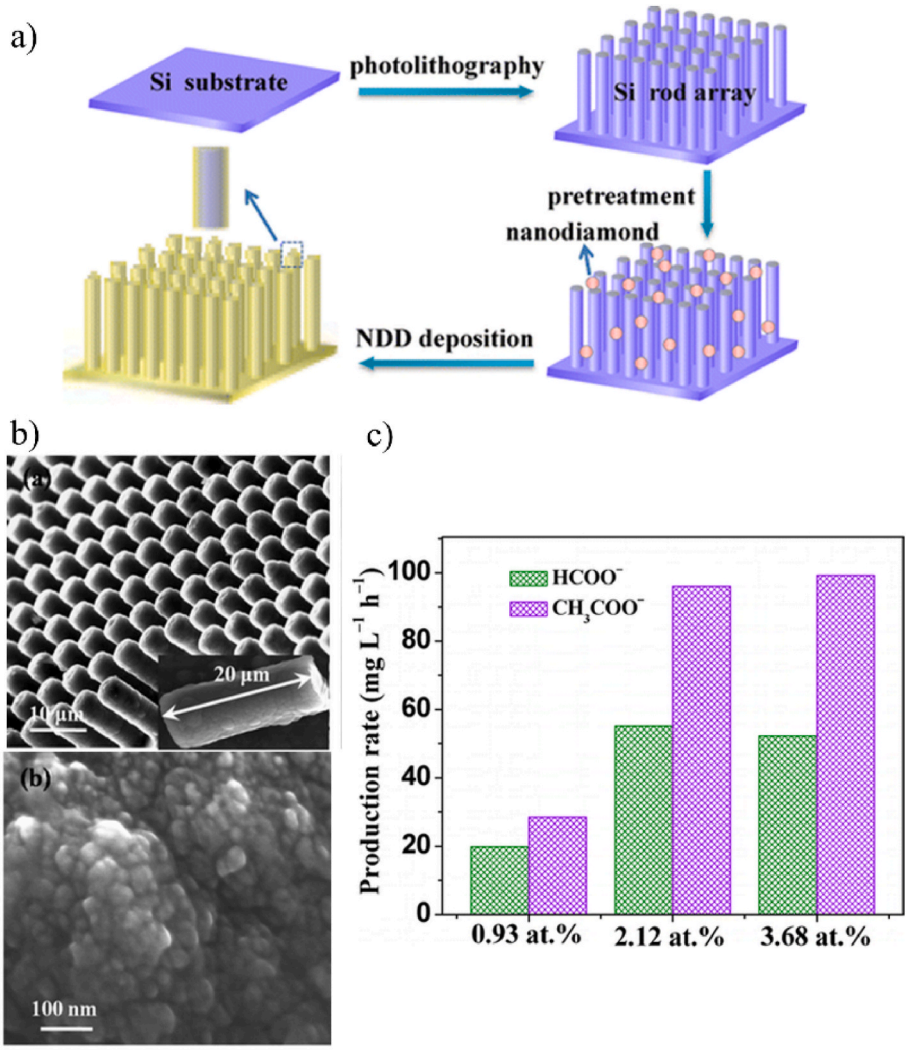

Fig. 11. a) Scheme of the NDD/Si RA preparation process, b) SEM images of NDD_L/Si RA. c) Acetate and formate production rates of acetate and formate on NDD_L/Si RA electrodes with different N contents (0.93, 2.12, and 3.68 atom %) at −1.0 V. Reprinted with permission from Ref. 123. Copyright © 2015 American Chemical Society.

that SiW_9V_3 was necessary for the acetic acid formation (as in the previous case using $SiW_{11}Mn$) and In for the CO_2 reduction since the first step on the mechanism was the In-facilitated formation of In–CO_3^- (instead of CO_2^{*-} intermediate). Besides, XPS spectra indicated that the V-center of SiW_9V_3 participates in the electron transfer process decreasing the overpotential, i.e., V-center efficiently catalyses the reduction of CO_2. Faradaic efficiencies in this system reached values up to 96% with nearly 96% selectivity towards acetic acid.

3.2. CO_2 to ethylene

The synthesis of C_{2+} products from CO_2, such as ethylene or ethanol, is of high importance due to the essential role of these products in the chemical and energy industry [119,181–183]. Ethylene is widely used as a building block in the production of many raw materials such as polyethylene, ethylene oxide, vinyl acetate, and ethylene glycol. Usually, ethylene is obtained from steam cracking of naphtha under harsh production conditions (800–900 °C). Although steam cracking is the industry standard for ethylene production, it presents different disadvantages. This process is non-catalytic and non-selective and is high energy and capital intensive, yielding into many by-products which require extensive separations and purification [184,185]. In recent years, the ethylene electrochemical synthesis from CO_2RR is gaining attention since this approach offers mild conditions and an environmental pathway for ethylene production [186,187]. However, the use of CO_2RR for the highly selective production of compounds of economic interest such as ethylene is still a challenge [186]. Concerning the catalyst, in the electrochemical environment of this reaction, i.e., abundant protons and negative electrode polarization, different catalytic behaviours have been observed: Ni, Fe, Pt, and Ti cathodes preferentially produce H_2 over CO/CO_2 production. Post-transition metals such as Pb, In, Sn, and Tl mostly produce formates. Additionally, Ag, Au, Pd and Zn reduce CO_2 only to CO. On the other hand, Cu possess the outstanding ability to reduce CO_2 or CO to CH_4, C_2H_4, C_2H_5OH, and a variety of products [188–190].

Copper catalysts have been extensively explored in the electrocatalytic synthesis of ethylene. It has been proved that tuning the intermediates' stabilities can favour a desirable reaction pathway and by consequence, improve the selectivity [190–192] However, the mechanistic pathway for the formation of ethylene over Cu catalyst is still under academic discussion [19]. While the C–C coupling of two carbenes ($*CH_2$) has been proposed as the determinant step for the synthesis of the C_2 product from CO_2RR over Cu catalyst [193], more recent, studies concluded that C_2 product formations are more attributed to CO dimerization.

Different theoretical and experimental studies have supported that

the CO dimerization pathway is the limiting step for ethylene production [192]. As shown in Fig. 12, in the CO dimerization, *CO + *CO (Fig. 12a), $*C_2O_2^-$ intermediate can exist either from carbon and oxygen atoms from $*C_2O_2^-$ intermediate, which are bounded to the catalyst surface in a bridging mode (Fig. 12b) or by the $*C_2O_2^-$ intermediate which is bounded to the surface by two C atoms (Fig. 12c). However, both ways proceed to further protonation of the $*C_2O_2^-$ intermediate giving place to more stable intermediates such as *CO–COH (Fig. 12d) of *COCHO [194]. Alternatively, Goodpaster et al. proposed that while at low overpotential, the formation of the C–C bond takes place in a reaction of two *CO bounded to the surface, at higher overpotential, the reaction between *CO and *CHO (Fig. 12e and f) is favoured as a result of the larger activation barrier to the formation of the CO dimer [195]. This intermediate is followed by the reaction with *CO to form *COCHO (Fig. 12g) and finally ethylene formation [164,165].

Copper has been selected as an ideal catalyst in the electrochemical conversion of CO_2 due to the thereof mentioned characteristics. Its reaction performance has been widely explored in CO_2RR by controlling morphology [113], grain boundaries [166], facets [196], oxidation states [197], molecule decoration [188–190], and dopants [198]. Among these methods, the design of Cu metallic nanostructures for C_{2+} products seems more promising due to the simple synthesis and the easy study of the structure-activity relationship of the catalyst. For instance, Roberts et al. showed that modifying the structure of the copper surface is a novel pathway to improve ethylene efficiency and selectivity. These authors obtained nanotubes-covered copper (CuCube) surface with high selectivity and low overpotential to ethylene formation, but also probed the effect of (100) sites in the C–C coupling as a strategy to target multicarbon products [199].

Recently Zhang et al. reported the design of Cu nanosheets as an electrocatalyst for ethylene synthesis from CO_2RR. These nanosheets (Fig. 13a) present defects in the size of 2–14 nm, which were observed to be strengths in the adsorption, enrichment, and confinement for reaction intermediates and hydroxyl ions on the catalyst. As shown in Fig. 13b, the maximum FE reached with these copper nanosheets was up to 83.2%, which is the highest value among all the studied electrocatalysts to date [200].

Loiudice et al. explored the effect of shape and size of Cu nanocrystals (NCs) in ethylene production. They explored crystal cube and spheres of Cu NCs, observing an increase in the activity as the crystal size decreased [116].

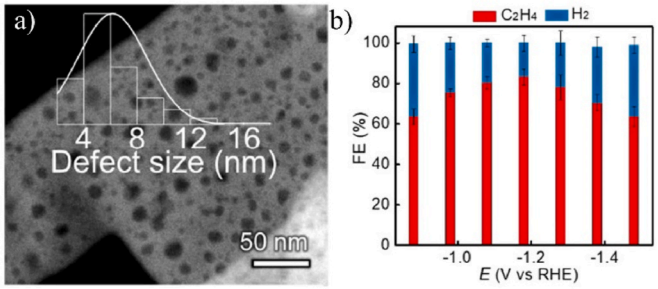

Fig. 13. a) HAADF-STEM images of n-CuNS and size distribution of the nanodefects b) Faradaic efficiencies of C_2H_4 and H_2 at different applied potentials for n-CuNS. Reprinted with permission from Ref. 200. Copyright © 2020 American Chemical Society.

The modification of oxidative copper states has also been proved to be an alternative to enhance the selectivity and efficiency of C_{2+} products [197,201]. Anodized-copper was investigated in CO_2RR as a tool to improve ethylene selectivity. It was observed that compared with a Cu foil, this anodized-Cu catalyst presented a two-fold improvement [202]. But most importantly, the selectivity continued stable over 40 h of the experiment. As it is observed in Fig. 14a, the catalyst performance remained stable, retaining an average of 38.1% FE for ethylene production. In this experiment, it was also observed the electrochemical treatment of the as-synthesized catalyst as a critical parameter in the ethylene selectivity (Fig. 14b). When the material was exposed to electrochemical reduction treatment at mild biased potential, the species were observed to suffer a reduction, quickly decreasing the ethylene selectivity. Meanwhile, when the treatment was performed at highly biased harsh conditions, the catalyst presents much extended durability for selectivity C–C coupling. These observations give evidence of the relationship between Cu–*O*-containing surface states and the durability of ethylene production, which are of high importance to develop new strategies for controlling selectivity and durability of O–Cu catalyst for electrochemical synthesis of ethylene [202].

The Cu-based alloys such as Ag–Cu, Au–Cu, Au–Pd, and Cu–Pt have

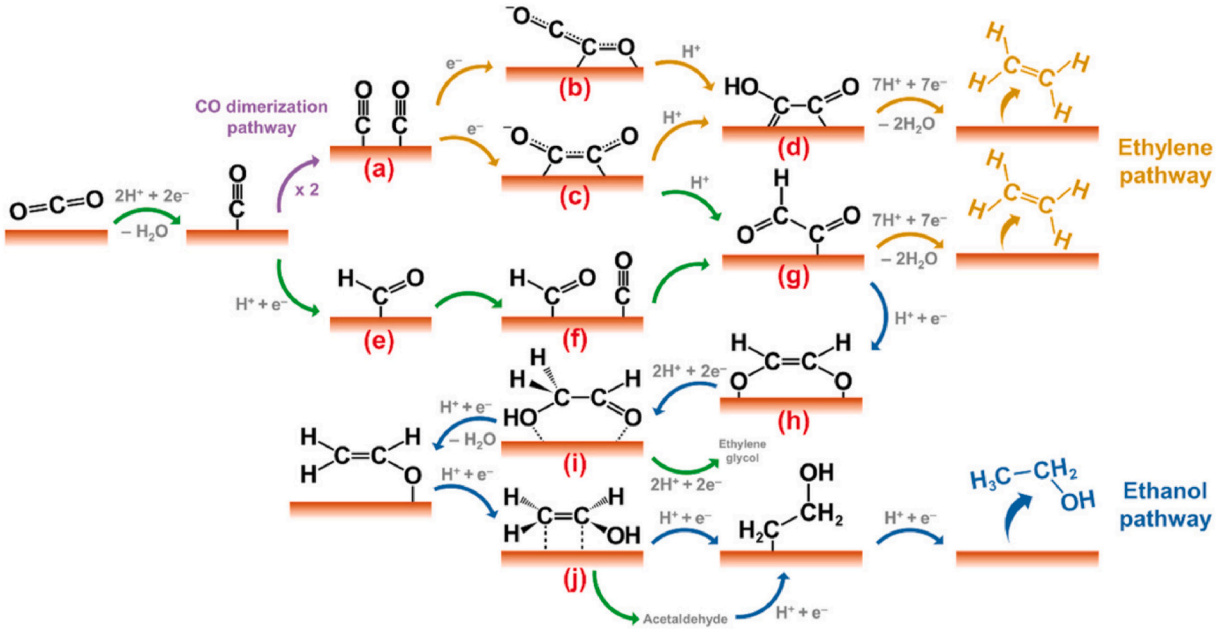

Fig. 12. Ethylene and ethanol formation. The brown and blue arrows indicate ethylene pathways and ethanol pathways. Reprinted with permission from Ref. 6. Copyright © 2020 WILEY-VCH Verlag GmbH & Co. KGaA, Weinheim.

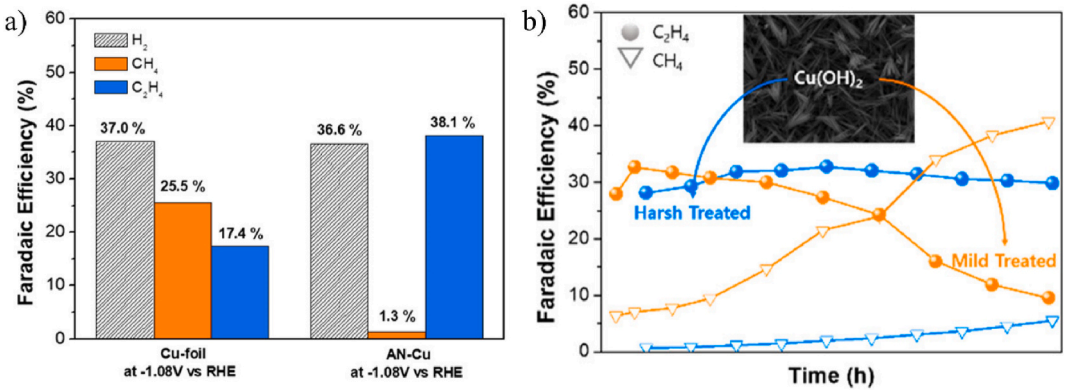

Fig. 14. a) Faradaic efficiencies of H_2, CH_4, and C_2H_4 at −1.08 V vs. RHE, b) Effect of the catalyst treatment in the FE of CH_4 and C_2H_4. Reprinted with permission from Ref. 202. Copyright © 2018 American Chemical Society.

been demonstrated to present a high efficiency in the C_1 production via stabilization of the intermediates [203,204]. However, the effect of these alloys in the production of C_{2+} hydrocarbons seem to be more complex [205]. For instance, Chang et al. reported an atomically dispersed Cu–Ag bimetallic catalyst where it was observed that Cu-rich zones preferred the production of hydrocarbons. In contrast, Ag-rich zones are dominated by CO. These experiments highlighted the importance of the atomic ratio for CO_2RR electrocatalysts [206]. Similar studies using Cu–Ag alloys from additive-controlled electrodeposition showed that Ag sites were believed to act as a promoter for CO formation during the electrocatalytic CO_2 reduction, helping the C–C coupling in the neighbouring Cu due to the availability of CO intermediate [207].

Molecular distribution in Pd–Cu catalyst has also proved to play an important role in improving the selectivity of C_{2+} compounds. For instance, Ma et al. demonstrated that a phase-separated Pd–Cu catalyst offered an ethylene selectivity up to 50% compared with its disordered

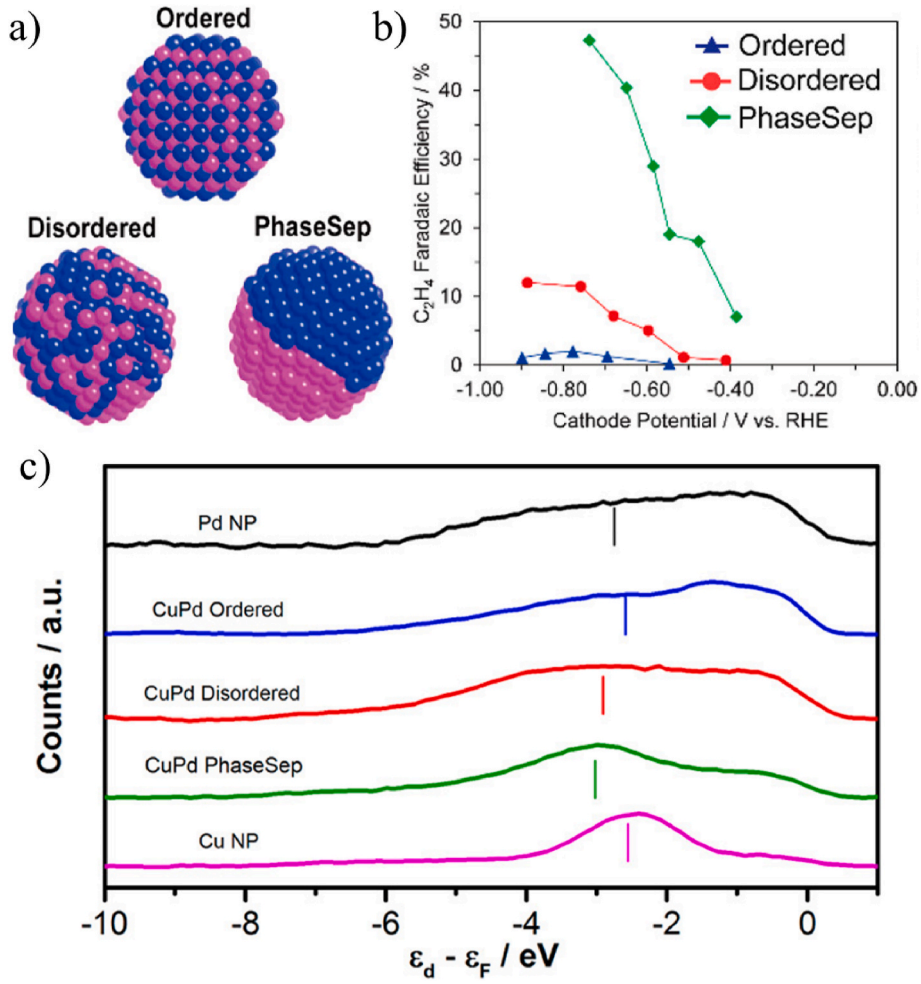

Fig. 15. a) Structures of the different prepared CuPd nanoalloys, b) Faradaic efficiencies for C_2H_4 formation using bimetallic Cu–Pd catalysts with different structures and c) Surface valence band photoemission spectra of CuPd nanoalloys corresponding to Fermi level. Reprinted with permission from Ref. 208. Copyright © 2016 American Chemical Society.

and ordered counterparts (Fig. 15a and b) [208]. Since according to the d-band theory, typically, lower d-band center transition metals show weaker binding on the in-situ generated intermediates on the metal surface [209]. The Pd–Cu alloy exhibited a similar catalytic activity and selectivity for CO that the ones obtained with Cu nanoparticles (NPs). It offered a wide d-band difference (Fig. 15c) which helps to conclude that the geometry and structure effect may play a more important role than the electronic effect for enhancing the selectivity of hydrocarbons in phase-separated Cu–Pd alloys case [208].

The nature of the electrocatalytic CO_2 reduction imposes the need of catalysts with specific active sites for the reactants adsorption and the further transformation of multiple intermediates, thus makes primary importance the increasing of specific active sites in the design of catalyst. As discussed in the oxalate section, MOFs have emerged as an alternative to act as both, as electrocatalysts or precursors to derive in different heterostructured catalysts due to their extraordinary properties and could be useful for electrochemical ethylene production from CO_2. In fact, from an electrochemical point of view, the permanent porosity, ultrahigh surface area, coordinatively unsaturated metal sites, adjustable pore size, and active sites homogeneous dispersion makes them highly attractive for this kind of reactions [210].

Post-synthesis modification of MOFs is a strategy of high relevance in the design of electrocatalysts since it could assemble the functional metal fractions such as metal porphyrin and metal complex that would enhance the CO_2 reduction in MOFs, particularly in those with coordinatively unsaturated metal sites, which interact with CO_2 working as Lewis acid [29,211,212]. Cu-BTC (HKUST-1), which presents open metal sites, has been widely studied in the CO_2RR due to its structural features that enhance the catalytic performance. Nam et al. reported the strategy involving the MOF-regulated Cu cluster formation (Fig. 16a) as a tool to optimize the selectivity of ethylene in comparison with MOF-based active carbon. They obtained an efficiency of up to 45% (Fig. 16b) [213].

MOFs derivates such as metal oxides, porous carbons, carbides, phosphides, and nitrides have appeared to overcome the main limitations of MOFs related to the poor stability and conductivity in electrochemical reactions [214–217]. For instance, Zheng et al. studied N-doped nanoporous carbon obtained from ZIF-8 for ERC, emphasizing the calcination temperature in the reaction and the mechanism. According to the catalytic performance, higher pyrolysis temperature resulted in a higher activity with a maximum FE for CO formation of 95.4% [218].

The design of atomically dispersed metals in activated carbon (AC) has also been a powerful tool in the electrochemical conversion of CO_2. As shown in Fig. 17, Guan et al. boosted the CO_2 electroreduction to CH_4 and C_2H_4 by tuning the neighbouring single-copper sites in a dopped-AC showing the Cu-coping concentration as a tool to direct the selectivity to the desired product. For instance, they showed that at a Cu high concentration, the distance between Cu-N_x species was close enough to enable C–C coupling and, by consequence, produce C_2H_4. In contrast, a

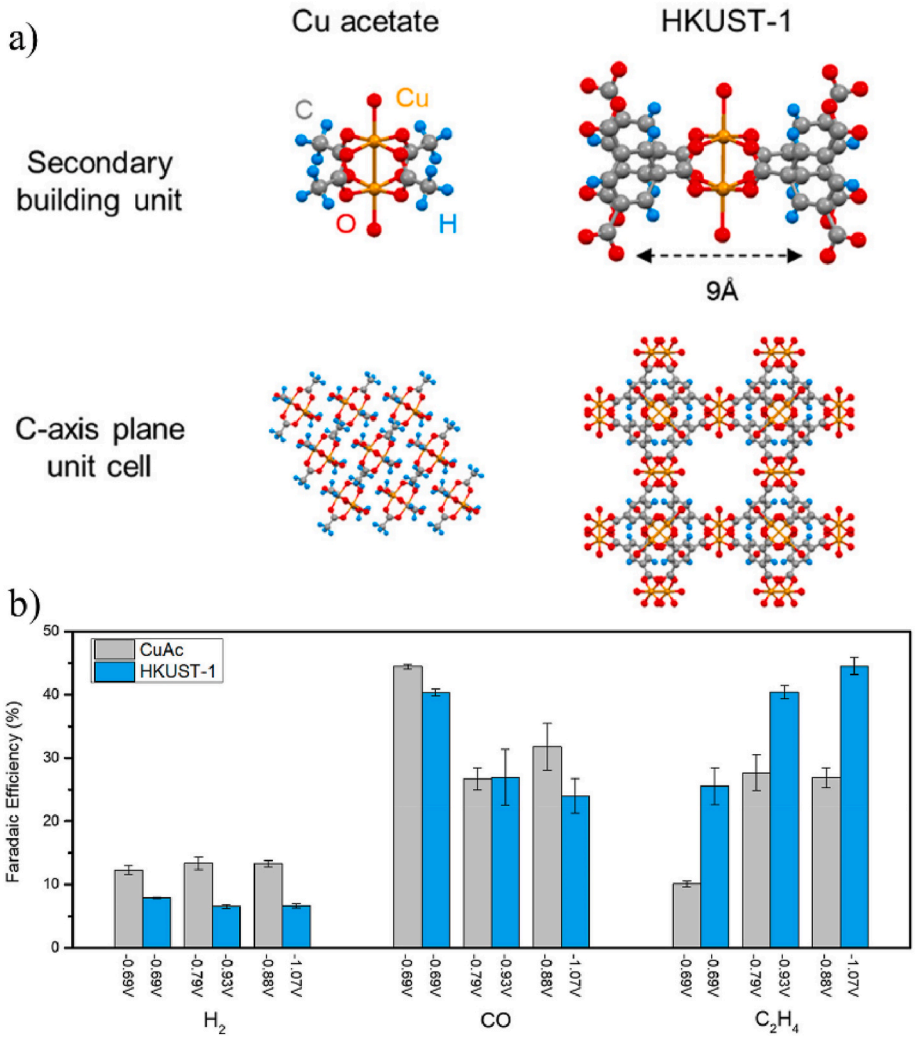

Fig. 16. a) Schematic Comparison of paddle-wheel structured HKUST-1 vs. CuAc. Structural investigations of as-fabricated HKUST-1, b) CO_2RR activities of CuAc (200 °C 1 h calcined), and HKUST-1 (250 °C 3 h calcined). Reprinted with permission from Ref. 213. Copyright © 2018 American Chemical Society.

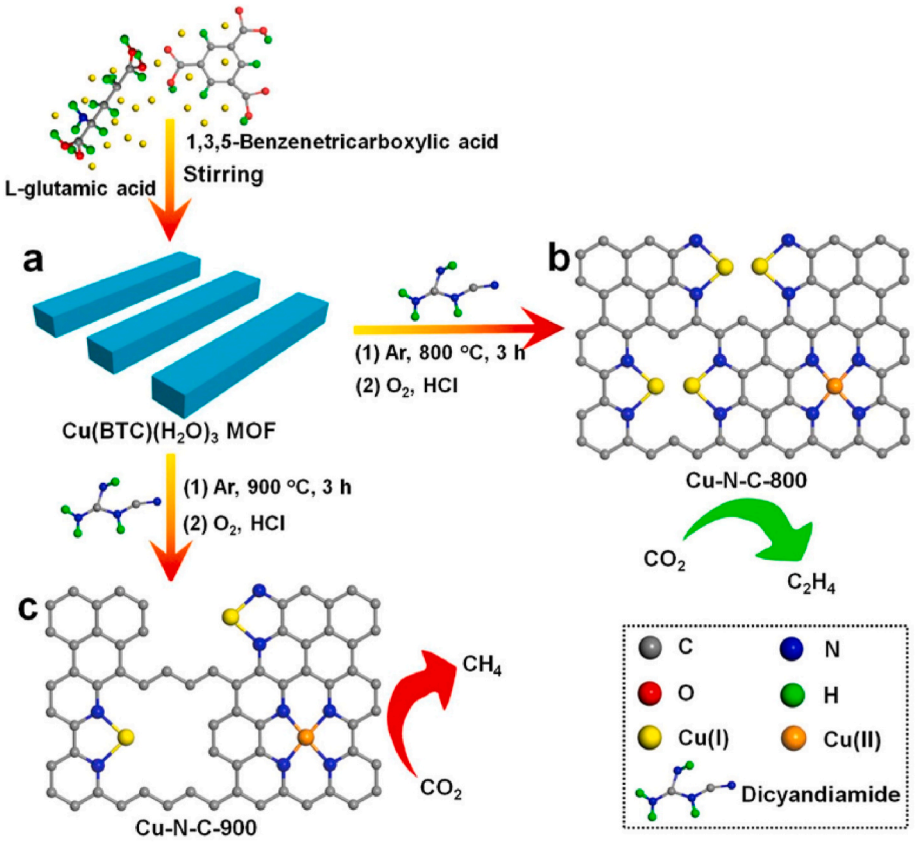

Fig. 17. Scheme of Cu–N–C-T catalysts synthesis process: a) Cu(BTC) $(H_2O)_3$ MOF precursor, b) Cu–N–C-800 synthesized by pyrolysis of Cu(BTC) $(H_2O)_3$ MOF and dicyandiamide at 800 °C, (c) Cu–N–C-900 derived from the pyrolysis of Cu(BTC) $(H_2O)_3$ MOF and dicyandiamide at 900 °C. Reprinted with permission from Ref. 219. Copyright © 2020 American Chemical Society.

Cu concentration lower than 2.4% mol, the distance between species was larger to the formation of CH_4 was favoured [219].

3.3. CO_2 to C_{2+} alcohols

The electrocatalytic conversion of CO_2 to higher-value hydrocarbons beyond the C_1 products is an area of extraordinary importance for applications such as transportation, fuels, energy storage, and the chemical industry [220]. With a worldwide production of ca. 88.5 Mt/y and a projection of US$105.2 billion by 2025, ethanol is an important organic chemical for the biofuel and food industries [221,222]. For instance, approximately 80% of global ethanol produced is used as fuel, followed by food, pharmaceutical, and cosmetics applications [223].

In recent years, electrochemical production of ethanol has been proposed as a green route to obtain this high-value chemical. As observed in Fig. 12, the electrochemical production of ethanol takes place in a similar pathway to ethylene, where the C–C coupling activity is considered a critical step in ethanol production, similarly to other C_{2+} products. Garza et al. proposed an ethanol pathway over Cu catalyst where it was observed that *COCHO intermediate (Fig. 12g) is the key to determinate the selectivity between ethylene and ethanol [165]. The glyoxal can be reduced to acetaldehyde and ethanol (Fig. 12h), followed by a further reduction to glycolaldehyde (Fig. 12i) and ethylene glycol/vinyl alcohol (Fig. 12j) or acetaldehyde, and finally to ethanol [164,189].

The main goal for CO_2RR to ethanol is to improve selectivity at high conversion rates, which are influenced by the catalyst and the process conditions. By far, Cu-based catalysts have been the most studied to catalyse CO_2RR for ethanol production [201,224,225]. In this sense and similarly to ethylene, different strategies have been studied to enhance ethanol selectivity in Cu-based catalysts, such as nanoparticle morphology [226,227], oxidation states [228], and Cu-based alloys [208,229]. For instance, Duan et al. studied the crystallinity of Cu nanoparticles as a driven parameter in the ethanol selectivity, observing that amorphous nanoparticles enhance the adsorption of CO_2 at room temperature, which plays a key role in the CO_2RR [230].

Several studies have demonstrated the strong relationship between product selectivity of CO_2RR and the crystal facets of Cu [231]. For example, Cu(100) increases the selectivity for ethylene, while in Cu (111) catalyst, methane is the main hydrocarbon product [67,115,116,232]. Jiang et al. developed and studied an efficient nanocube-shaped catalyst with significant improvement in C_{2+} selectivity. It was reported that Cu(100) and (211) facets favour ethanol and other C_{2+} products over Cu(111) via dimerization of *CO to form *OCCO and the subsequent proton-electron transfer and surface hydrogenation to form *OCCHO [196].

The oxidation states of copper can vary among Cu_0, Cu^+, and Cu^{2+}, and their states change reversibly during electrochemical reaction conditions. Copper oxide-based catalysts improve the activity and selectivity of C_{2+} products. Generally, copper oxide-based catalysts are synthesized by the growing of Cu_2O from Cu-based precursors followed by high-temperature treatment and consequently reducing Cu_2O to form Cu_0 sites. However, the elucidation of the pathways of this enhancement toward C_2 formation is still under debate [19]. Tentatively, the enhancement of the selectivity for ethanol of such catalyst could be attributed to (i) the presence of residual oxygen atoms close to the surface that favour the modification of the electronic structure of Cu atoms and the increase of the CO binding energy, which by consequence promotes C–C couplings [233]; (ii) the strong adsorption of H_2O molecules due to the presence of residual Cu^+ which may work synergically with Cu_0 sites. These H_2O molecules favour the CO_2 conversion to CO [117,118]. For instance, Handoko et al. reported a mechanistic study

electroreduction of CO_2 to ethanol and other C_{2+} hydrocarbons on Cu_2O-derived films. They synthesized Cu_2O films with five different morphologies and proved a relationship between the crystal size and the selectivity to C_2 products being able to reach a FE of c. a. 20% in middle-sized particles [234].

A wide variety of morphologies of copper oxide-based materials has been reported as a determinant factor to enhance ethanol production. For instance, Daiyan et al. reported the synthesis of nanowires of Cu_2O/CuO/Cu foam (Fig. 18a) that exhibited a FE for ethanol formation of 31% [235]. Also, 3D dendritic Cu–Cu_2O/Cu catalyst (Fig. 18b) were synthesized and proved a FE up to 39.2% attributed to the high density of exposed active sites and favourable Cu_2O:Cu ratio [220].

Copper alloys have attracted considerable attention as a strategy to change the composition of Cu single crystal catalysts via combining it with a secondary metal able to produce H_2 (i.e., Fe, Ni, Ag, Au, and Pd) and to tune the activity and selectivity through optimization of the binding strength of the key intermediates on the surface of the catalyst [6]. For instance, Shen et al. described the synthesis of submicron arrays based on the alloy CuAu reaching a FE up to 29%. It showed the critical role of Cu:Au ratio content in the selectivity ethanol/ethylene [236]. Interestingly, in the same way as metal ratios, the phase distribution of the metal involved in the alloys has been proved to be a determinant factor in directing the selectivity to ethylene or ethanol. As observed in Fig. 19a, which shows the ethanol/ethylene selectivity in an Cu/Ag catalyst, the selectivity is three times higher in the catalyst with phase blended, probably related to the effect of the dopant in the surrounding Cu atoms but also to the effect of Ag–Cu biface boundaries that suppresses the HER and favours the formation of mobile CO on Ag sites and its further reaction to a residual intermediate on Cu sites (Fig. 19b and c) [225].

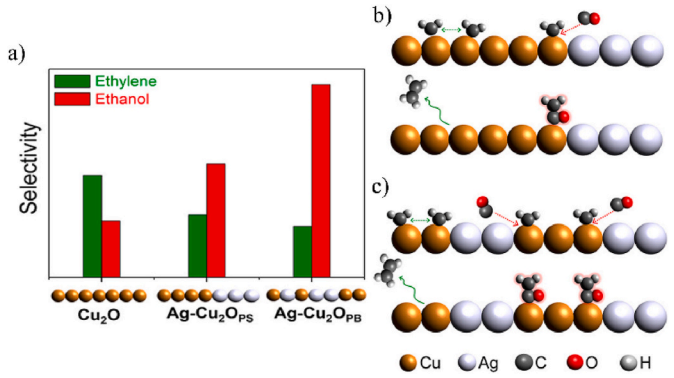

Fig. 19. a) Ethylene and ethanol selectivity in Cu/Ag catalyst. Possible CO-insertion reaction mechanism scheme: CO transfer from one metal site that weakly binds CO (Ag) to another site that binds residual C_1 intermediate species (Cu) for the case of b) Ag–Cu_2OPS and c) Ag–Cu_2OPB. Reprinted with permission from Ref. 225. Copyright © 2017 American Chemical Society.

In the last decade, MOFs, and especially those formed by Cu metal ions or clusters, have served as active electrocatalyst in CO_2RR but also as precursors for highly dispersed Cu over N-doped carbon catalysts [237,238]. For instance, Zhao et al. synthesized a porous Cu/C catalyst consisting of Cu_2O and metal Cu particles embedded in a porous carbon matrix through the pyrolysis of Cu-based MOF (HKUST-1) (Fig. 20). A maximum FE for ethanol production of 34.8% at a potential of −0.5 V was obtained using this selective catalyst [239].

The electrochemical reduction of CO_2 to C_{3+} products remains a challenge. Among the C_1–C_3 alcohols, n-propanol possesses the highest

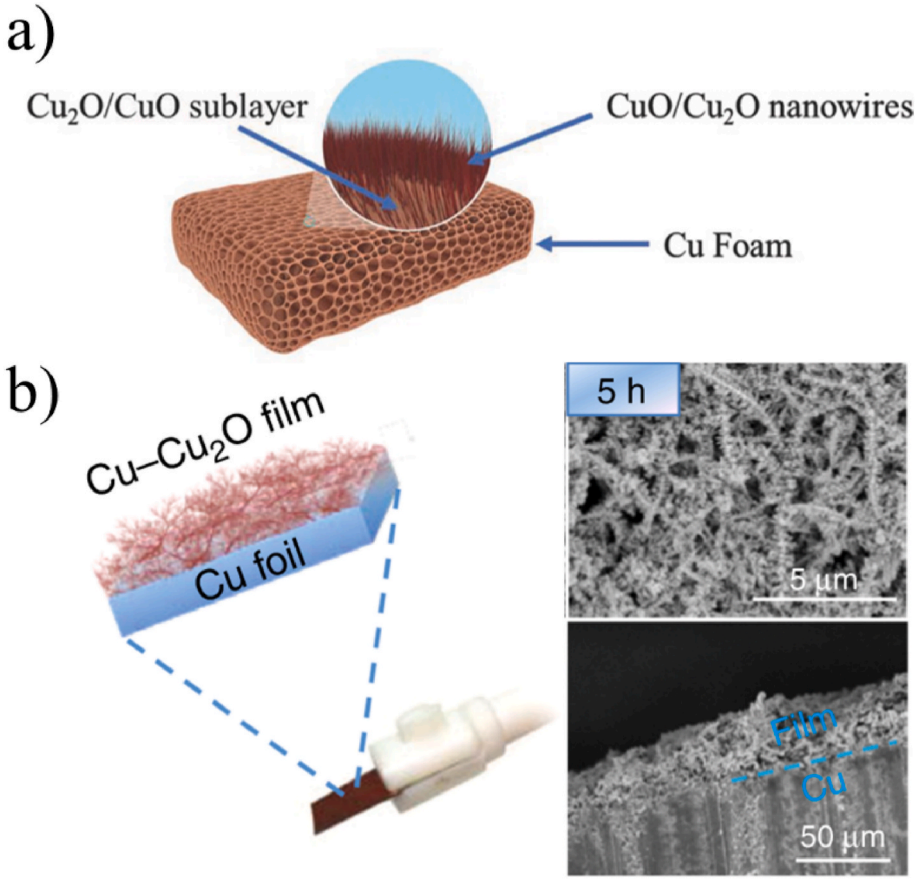

Fig. 18. a) Scheme of Cu sandwich electrode. Reprinted with permission from Ref. 203. Copyright © 2018 WILEY-VCH Verlag GmbH & Co. KGaA, Weinheim. b) Scheme of 3D dendritic catalyst and SEM images of the catalyst. Reprinted with permission from Ref. 220. Copyright © 2019, Qinggong Zhu et al.

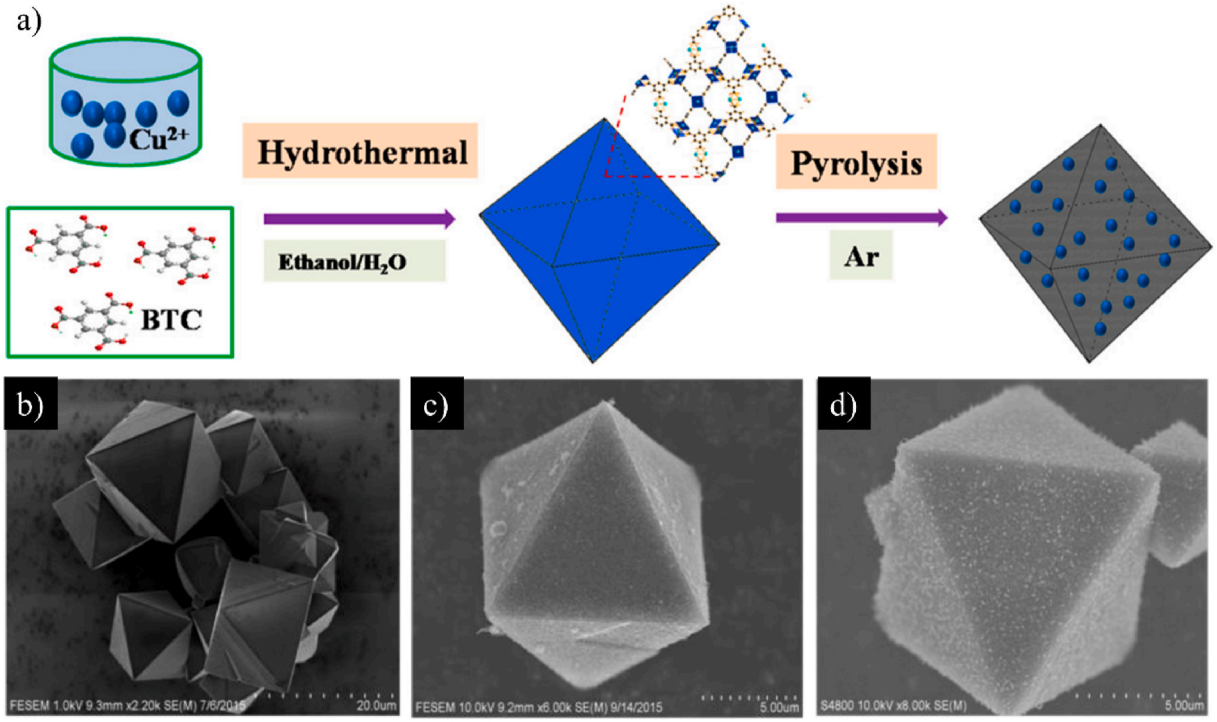

Fig. 20. a) Scheme of synthesis of HKUST-1 and Cu/C electrocatalyst and b) SEM image of HKUST-1 crystals, c) SEM image of Cu/C catalyst treated at 900 °C, and d) SEM image of Cu/C catalyst treated at 100 °C. Reprinted with permission from Ref. 239. Copyright © 2017 American Chemical Society.

energy-mass density (30.94 kJ/g) and an octane number up to 118 [240, 241]. These relevant properties make the efficient and green production of n-propanol a target point nowadays.

The n-propanol production by a CO_2 reduction reaction has been only observed in Cu-based catalysts. It has been hypothesized the pathways for n-propanol production as a result of the transformation of acetaldehyde into vinyl alcohol by a tautomerization equilibrium [227, 242]. As observed in Fig. 21, the adjacent intermediates CO and $*CH_2$ are inserted into $*CH_3$–CH in a similar way. Then, the reduction to propionaldehyde (CH_3–CH_2–CHO) and, consequently, to n-propanol takes place [20].

Ren et al. reported a mechanistic study to n-propanol electrosynthesis via the design of nanocrystals agglomerates with unprecedented catalytic activity. The defect sites generated in the catalyst surface was responsible for the improved activity of the Cu nanocrystals and, hence, the n-propanol formation [227].

4. Market perspective and techno-economic aspects

In contrast with the previous sections, in which each product has been reviewed separately, here we give a general overview of the market aspects and techno-economic analysis carried out to date. The market size of the targeted products is critical from both a commercial perspective and CO_2 utilization potential. In this vein, Fig. 22 presents the approximate market size of the C_2-products here considered [243–249]. As shown, for example, propanol and acetic acid market sizes are very low in comparison with other potential CO_2 utilization routes. For instance, other relevant CO_2 utilization alternatives such as $CaCO_3$ production, have a market sizes one hundred times higher than propanol and acetic acid (116 Mton/a market size) [250]. Nonetheless, their production from CO_2 should not be dismissed as the production capacities may fit with the capacities of small-medium CO_2 emitters. A fair example of these emitters is biogas upgrading, that could achieve the category of negative CO_2 emissions technology if propanol or acetic acid are produced from the CO_2 contained in this bio-resource. Oxalic acid is a very interesting C_2 product from a utilization perspective since it is

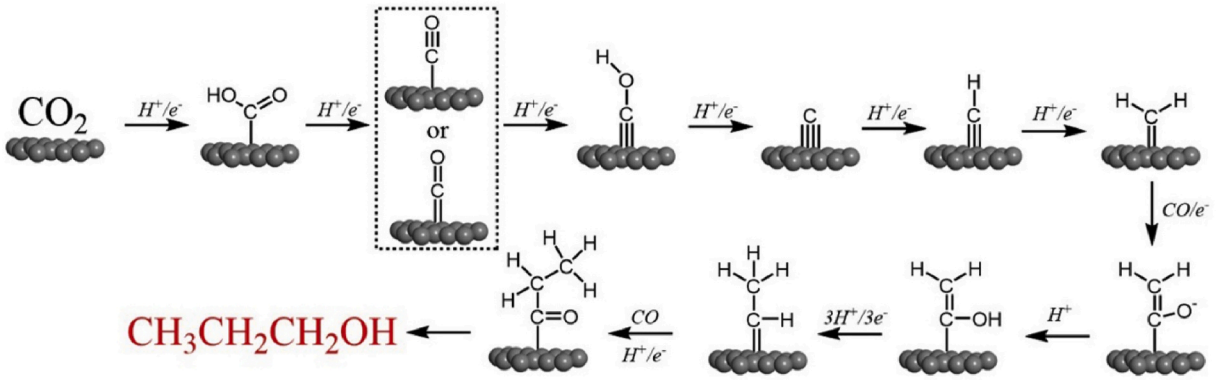

Fig. 21. Possible pathway to n-propanol production via CO_2 reduction reaction. Reprinted with permission from Ref. 20. Copyright © 2018 Elsevier Ltd.

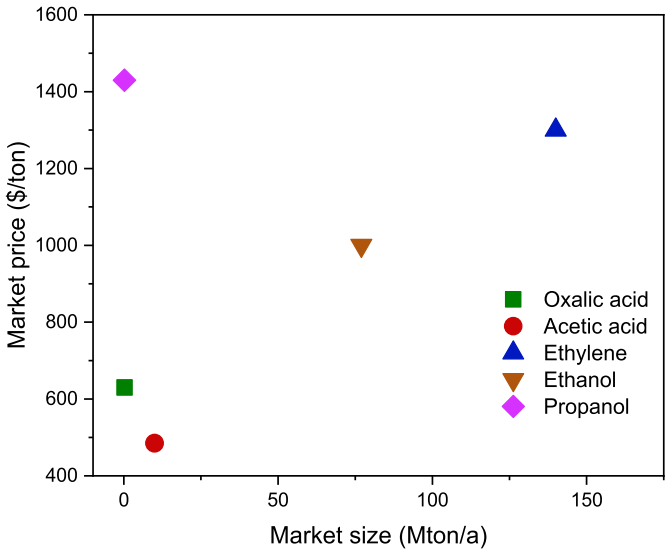

Fig. 22. Market size vs market price for C_2 products [213–219].

demanded by pharmaceuticals, textiles manufacturing, rare earth extraction, oil refining or metal processing industries. Nonetheless, worldwide oxalic acid production is above 0.230 Mton/a [249], which places oxalic acid in the same range than propanol and acetic acid. Therefore, this option cannot provide an alternative for CO_2 utilization of large emitters. Ethylene and ethanol present market sizes considerably greater, and as explained in previous sections, the production of these chemicals is crucial for the end-products consumed by our society nowadays.

On the other hand, Fig. 22 also presents the market prices for the products studied. From a market price point of view, ethanol, ethylene and propanol are the most attractive products to be achieved via CO_2 electrocatalytic reduction. Although rapidly booming, CO_2 utilization technologies are currently far from being competitive with traditional technologies, hence focusing on products with elevated market prices could be a good strategy to balance economic performance. Following this reasoning, the production of oxalic and acetic acid from CO_2 would be difficult to become economically profitable with the current market prices in the short term. However, the growing projection for CO_2 emission taxes along with the ongoing commitments to pursue a net-zero emissions opens the possibility for the viable production of all these chemicals using electrochemical routes.

Concerning techno-economic works carried out to date, only a few studies are reported in literature. Economic assessment of CO_2 electrocatalytic reduction are scarce probably because of the complexity of the analysis and the lack of reliable commercial scale data. In this sense, this criticism aims to be an encouraging call for experts in techno-economic and profitability evaluations. Focusing on the works performed, Table 1 gathers the most important characteristics and findings of the techno-economic analysis available in the literature. Perhaps the most impacting study carried out to date was performed by Jouny et al. [243] In this work, authors present the end-of-life net present value (NPV) of a 100 ton/day plant for various CO_2 reduced products: propanol, formic acid, carbon monoxide, ethanol, ethylene and methanol. From the products targeted in their study, here we focus on propanol, ethanol and ethylene. Under the current conditions, authors conclude that the production of these C_2-products from CO_2 is not profitable. Nevertheless, the result could be reverted if reasonable electrocatalytic performance benchmarks are achieved. In agreement with these authors, these performances must be 300 mA cm^{-2} and 0.5 V overpotential at 70% FE. Another very important work was presented by Kibria et al. [244]. In their work, a techno-economic analysis was carried out with the aim of ensuring the economic viability of the process by the identification of profitable CO_2 electrocatalytic reduced products as well as the performance targets that should be met to achieve it. As in the previous discussed work, this study includes parameters such as current density, energy and faradaic efficiencies, and stability. The most interesting point of this work is the prices predicted for ethanol and ethylene to achieve profitable scenarios. According to these authors analysis, ethanol price should achieve 1400 $/ton to get a net present value equal to zero (revenues equal to costs at the end of the plant life). In comparison with the current market price for ethanol (around 1000 $/ton, see Fig. 22), the difference is 40%. This fact shows the great technological challenge that we face to make electrocatalysis economically attractive in the context of direct CO_2 conversion to C_2 products. In the same study, a price of 1700 $/ton is predicted for ethylene to be a profitable alternative. Again, in comparison with current market prices (approximately 1300 $/ton), the threshold needed is remarkably higher. Interestingly, the authors present a sensitivity analysis based on a tornado plot, revealing that current density is the main parameter with room for improvement for all the products considered.

5. Final remarks and outlook

The transition towards sustainable modern societies relies on the implementation of disruptive technologies for CO_2 utilization. Among these technologies, electrocatalytic CO_2 conversion to added value products will play a major role given its advantages compared to traditional thermal catalysis. In particular, the fact the electrochemical reactions can take place at very mild conditions represents a major bright side of this approach. So far, most the academic works are focused on the conversion of CO_2 to C_1 products since the reaction is "electrochemically cheaper". Nevertheless, the production of C_2 and C_{2+} is more appealing for the chemical industry given the broad market applications of these advanced products. Herein, challenges on the catalysts design to achieve high faradaic efficiencies and end-product selectivity are identified as the main bottlenecks for the electrochemical CO_2 conversion to C_2 and C_{2+} compounds. Among the different studied heterogenous catalysts, Cu-based formulations outstand showcasing the best activity/selectivity balance. However, in many cases their performance is still below the threshold to be considered as commercially viable options. In this sense, new formulations of advanced materials including multi-alloy systems, N-doped catalysts, optimized porous MOFs structures among many others are under development showing promising results. In this sense, our review provides an end-product guided perspective of the progress within catalyst design to deliver C_2 and C_{2+} from electrochemical CO_2 conversion routes. Beyond offering an illustrative analysis for experts and a straightforward starting point to newcomers in the field, our work would also like to emphasize the need to strengthen the research efforts within the catalysis and energy communities in the conversion of CO_2 to advanced products. More precisely we advocate for a C_2 and C_{2+} production using a new generation of advanced electrocatalytic materials.

Along with the catalysts design and electrochemical processes considerations, market studies are crucial to ascertain the viability of the CO_2 electrochemical conversion routes. Our analysis indicates that products with a broad market such as ethanol, ethylene and propanol are worth exploring in the short term while electrochemical production of other key products such as oxalic and acetic acids are not yet economically appealing. Still, progress on catalyst design pushing forward products selectivity and overall CO_2 conversion will certainly help to make these options also viable. In any case, the production of advanced products using CO_2 as carbon pool and electrocatalysts design seem to share a common destiny whose convergence will result in a remarkable contribution to decarbonise the chemical industry, opening new routes for the desired low-carbon future.

Author contributions

The authors equally contributed to this work.

Declaration of competing interest

The authors declare that they have no known competing financial interests or personal relationships that could have appeared to influence the work reported in this paper.

Acknowledgements

Financial support for this work was gathered from Spanish Ministry of Science and Spanish Ministry of Science and Innovation through the projects RTI2018-096294-B-C33 and RYC2018-024387-I. This work was also partially funded by the University of Seville via the VI PPIT grant scheme for talented researchers. Support from CO2Chem UK through the EPSRC grant EP/P026435/1 is also acknowledged. Financial support from the European Commission through the H2020-MSCA-RISE-2020 BIOALL project (Grant Agreement: 101008058) is also acknowledge.

References

[1] Gao W, Liang S, Wang R, Jiang Q, Zhang Y, Zheng Q, et al. Industrial carbon dioxide capture and utilization: state of the art and future challenges. Chem Soc Rev 2020;49:8584–686. https://doi.org/10.1039/d0cs00025f.
[2] Mikkelsen M, Jørgensen M, Krebs FC. The teraton challenge. A review of fixation and transformation of carbon dioxide. Energy Environ Sci 2010;3:43–81. https://doi.org/10.1039/b912904a.
[3] Zhu DD, Liu JL, Qiao SZ. Recent advances in inorganic heterogeneous electrocatalysts for reduction of carbon dioxide. Adv Mater 2016;28:3423–52. https://doi.org/10.1002/adma.201504766.
[4] Li K, Peng B, Peng T. Recent advances in heterogeneous photocatalytic CO2 conversion to solar fuels. ACS Catal 2016;6:7485–527. https://doi.org/10.1021/acscatal.6b02089.
[5] Alper E, Yuksel Orhan O. CO2 utilization: developments in conversion processes. Petroleum 2017;3:109–26. https://doi.org/10.1016/j.petlm.2016.11.003.
[6] Tomboc GM, Choi S, Kwon T, Hwang YJ, Lee K. Potential link between Cu surface and selective CO2 electroreduction: perspective on future electrocatalyst designs. Adv Mater 2020;32:1908398. https://doi.org/10.1002/adma.201908398.
[7] Kamkeng ADN, Wang M, Hu J, Du W, Qian F. Transformation technologies for CO2 utilisation: current status, challenges and future prospects. Chem Eng J 2021;409:128138. https://doi.org/10.1016/j.cej.2020.128138.
[8] Yaashikaa PR, Senthil Kumar P, Varjani SJ, Saravanan A. A review on photochemical, biochemical and electrochemical transformation of CO2 into value-added products. J CO2 Util 2019;33:131–47. https://doi.org/10.1016/j.jcou.2019.05.017.
[9] Mustafa A, Lougou BG, Shuai Y, Wang Z, Tan H. Current technology development for CO2 utilization into solar fuels and chemicals: a review. J Energy Chem 2020;49:96–123. https://doi.org/10.1016/j.jechem.2020.01.023.
[10] Xie H, Wang T, Liang J, Li Q, Sun S. Cu-based nanocatalysts for electrochemical reduction of CO2. Nano Today 2018;21:41–54. https://doi.org/10.1016/j.nantod.2018.05.001.
[11] Wang X, Zhao Q, Yang B, Li Z, Bo Z, Lam KH, et al. Emerging nanostructured carbon-based non-precious metal electrocatalysts for selective electrochemical CO2 reduction to CO. J Mater Chem 2019;7:25191–202. https://doi.org/10.1039/c9ta09681g.
[12] Ganji P, Borse RA, Xie J, Mohamed AGA, Wang Y. Toward commercial carbon dioxide electrolysis. Adv Sustain Syst 2020;4:2000096. https://doi.org/10.1002/adsu.202000096.
[13] Fan L, Xia C, Yang F, Wang J, Wang H, Lu Y. Strategies in catalysts and electrolyzer design for electrochemical CO2 reduction toward C2+ products. Sci Adv 2020;6. https://doi.org/10.1126/sciadv.aay3111. eaay3111.
[14] Marepally BC, Ampelli C, Genovese C, Saboo T, Perathoner S, Wisser FM, et al. Enhanced formation of >C1 products in electroreduction of CO2 by adding a CO2 adsorption component to a gas-diffusion layer-type catalytic electrode. ChemSusChem 2017;10:4442–6. https://doi.org/10.1002/cssc.201701506.
[15] Zha B, Li C, Li J. Efficient electrochemical reduction of CO2 into formate and acetate in polyoxometalate catholyte with indium catalyst. J Catal 2020;382:69–76. https://doi.org/10.1016/j.jcat.2019.12.010.
[16] Genovese C, Ampelli C, Perathoner S, Centi G. Mechanism of C-C bond formation in the electrocatalytic reduction of CO2 to acetic acid. A challenging reaction to use renewable energy with chemistry. Green Chem 2017;19:2406–15. https://doi.org/10.1039/c6gc03422e.
[17] Prieto G. Carbon dioxide hydrogenation into higher hydrocarbons and oxygenates: thermodynamic and kinetic bounds and progress with heterogeneous and homogeneous catalysis. ChemSusChem 2017;10:1056–70. https://doi.org/10.1002/cssc.201601591.
[18] Albo J, Alvarez-Guerra M, Castaño P, Irabien A. Towards the electrochemical conversion of carbon dioxide into methanol. Green Chem 2015;17:2304–24. https://doi.org/10.1039/c4gc02453b.
[19] Zheng Y, Vasileff A, Zhou X, Jiao Y, Jaroniec M, Qiao SZ. Understanding the roadmap for electrochemical reduction of CO2 to multi-carbon oxygenates and hydrocarbons on copper-based catalysts. J Am Chem Soc 2019;141:7646–59. https://doi.org/10.1021/jacs.9b02124.
[20] Fan Q, Zhang M, Jia M, Liu S, Qiu J, Sun Z. Electrochemical CO2 reduction to C2 + species: heterogeneous electrocatalysts, reaction pathways, and optimization strategies. Mater Today Energy 2018;10:280–301. https://doi.org/10.1016/j.mtener.2018.10.003.
[21] Spurgeon JM, Kumar B. A comparative technoeconomic analysis of pathways for commercial electrochemical CO2 reduction to liquid products. Energy Environ Sci 2018;11:1536–51. https://doi.org/10.1039/c8ee00097b.
[22] Lin R, Guo J, Li X, Patel P, Seifitokaldani A. Electrochemical reactors for CO2 conversion. Catalysts 2020;10:473. https://doi.org/10.3390/catal10050473.
[23] Malkhandi S, Yeo BS. Electrochemical conversion of carbon dioxide to high value chemicals using gas-diffusion electrodes. Curr Opin Chem Eng 2019;26:112–21. https://doi.org/10.1016/j.coche.2019.09.008.
[24] Verma S, Kim B, Jhong HRM, Ma S, Kenis PJA. A gross-margin model for defining technoeconomic benchmarks in the electroreduction of CO2. ChemSusChem 2016;9. https://doi.org/10.1002/cssc.201600394. 1972–9.
[25] Song JT, Song H, Kim B, Oh J. Towards higher rate electrochemical CO 2 conversion: from liquid-phase to gas-phase systems. Catalysts 2019;9:224. https://doi.org/10.3390/catal9030224.
[26] Yin Z, Palmore GTR, Sun S. Electrochemical reduction of CO2 catalyzed by metal nanocatalysts. Trends Chem 2019;1:739–50. https://doi.org/10.1016/j.trechm.2019.05.004.
[27] Hou L, Yan J, Takele L, Wang Y, Yan X, Gao Y. Current progress of metallic and carbon-based nanostructure catalysts towards the electrochemical reduction of CO 2. Inorg Chem Front 2019;6:3363–80. https://doi.org/10.1039/c9qi00484j.
[28] Nguyen DLT, Kim Y, Hwang YJ, Won DH. Progress in development of electrocatalyst for CO 2 conversion to selective CO production. Carbon Energy 2020;2:72–98. https://doi.org/10.1002/cey2.27.
[29] Kortlever R, Shen J, Schouten KJP, Calle-Vallejo F, Koper MTM. Catalysts and reaction pathways for the electrochemical reduction of carbon dioxide. J Phys Chem Lett 2015;6:4073–82. https://doi.org/10.1021/acs.jpclett.5b01559.
[30] Nitopi S, Bertheussen E, Scott SB, Liu X, Engstfeld AK, Horch S, et al. Progress and perspectives of electrochemical CO2 reduction on copper in aqueous electrolyte. Chem Rev 2019;119:7610–72. https://doi.org/10.1021/acs.chemrev.8b00705.
[31] Liu A, Gao M, Ren X, Meng F, Yang Y, Gao L, et al. Current progress in electrocatalytic carbon dioxide reduction to fuels on heterogeneous catalysts. J Mater Chem 2020;8:3541–62. https://doi.org/10.1039/c9ta11966c.
[32] Birdja YY, Pérez-Gallent E, Figueiredo MC, Göttle AJ, Calle-Vallejo F, Koper MTM. Advances and challenges in understanding the electrocatalytic conversion of carbon dioxide to fuels. Nat Energy 2019;4:732–45. https://doi.org/10.1038/s41560-019-0450-y.
[33] Oldham KB. A Gouy-Chapman-Stern model of the double layer at a (metal)/(ionic liquid) interface. J Electroanal Chem 2008;613:131–8. https://doi.org/10.1016/j.jelechem.2007.10.017.
[34] Zhang L, Zhao ZJ, Gong J. Nanostructured materials for heterogeneous electrocatalytic CO2 reduction and their related reaction mechanisms. Angew Chem Int Ed 2017;56:11326–53. https://doi.org/10.1002/anie.201612214.
[35] Gabardo CM, Seifitokaldani A, Edwards JP, Dinh CT, Burdyny T, Kibria MG, et al. Combined high alkalinity and pressurization enable efficient CO2 electroreduction to CO. Energy Environ Sci 2018;11:2531–9. https://doi.org/10.1039/c8ee01684d.
[36] Burdyny T, Smith WA. CO2 reduction on gas-diffusion electrodes and why catalytic performance must be assessed at commercially-relevant conditions. Energy Environ Sci 2019;12:1442–53. https://doi.org/10.1039/c8ee03134g.
[37] Verma S, Lu X, Ma S, Masel RI, Kenis PJA. The effect of electrolyte composition on the electroreduction of CO2 to CO on Ag based gas diffusion electrodes. Phys Chem Chem Phys 2016;18:7075–84. https://doi.org/10.1039/c5cp05665a.
[38] Marcus Y. Solubility parameter of carbon dioxide-an enigma. ACS Omega 2018;3:524–8. https://doi.org/10.1021/acsomega.7b01665.
[39] Zhao SF, Horne M, Bond AM, Zhang J. Is the imidazolium cation a unique promoter for electrocatalytic reduction of carbon dioxide? J Phys Chem C 2016;120:23989–4001. https://doi.org/10.1021/acs.jpcc.6b08182.
[40] Hollingsworth N, Taylor SFR, Galante MT, Jacquemin J, Longo C, Holt KB, et al. Reduction of carbon dioxide to formate at low overpotential using a superbase ionic liquid. Angew Chem Int Ed 2015;54:14164–8. https://doi.org/10.1002/anie.201507629.
[41] Lau GPS, Schreier M, Vasilyev D, Scopelliti R, Grätzel M, Dyson PJ. New insights into the role of imidazolium-based promoters for the electroreduction of CO2 on a silver electrode. J Am Chem Soc 2016;138:7820–3. https://doi.org/10.1021/jacs.6b03366.
[42] Garg S, Li M, Weber AZ, Ge L, Li L, Rudolph V, et al. Advances and challenges in electrochemical CO2 reduction processes: an engineering and design perspective looking beyond new catalyst materials. J Mater Chem 2020;8:1511–44. https://doi.org/10.1039/c9ta13298h.
[43] Rosen BA, Hod I. Tunable molecular-scale materials for catalyzing the low-overpotential electrochemical conversion of CO2. Adv Mater 2018;30:1706238. https://doi.org/10.1002/adma.201706238.
[44] Medina-Ramos J, Zhang W, Yoon K, Bai P, Chemburkar A, Tang W, et al. Cathodic corrosion at the bismuth-ionic liquid electrolyte interface under conditions for

CO2 reduction. Chem Mater 2018;30:2362–73. https://doi.org/10.1021/acs.chemmater.8b00050.
[45] Clark EL, Resasco J, Landers A, Lin J, Chung LT, Walton A, et al. Standards and protocols for data acquisition and reporting for studies of the electrochemical reduction of carbon dioxide. ACS Catal 2018;8:6560–70. https://doi.org/10.1021/acscatal.8b01340.
[46] Wuttig A, Surendranath Y. Impurity ion complexation enhances carbon dioxide reduction catalysis. ACS Catal 2015;5:4479–84. https://doi.org/10.1021/acscatal.5b00808.
[47] Guo W, Liu S, Tan X, Wu R, Yan X, Chen C, et al. Highly efficient CO2 electroreduction to methanol through atomically dispersed Sn coupled with defective CuO catalysts. Angew Chem Int Ed 2021;60. https://doi.org/10.1002/anie.202108635. 21979–87.
[48] Feng J, Gao H, Zheng L, Chen Z, Zeng S, Jiang C, et al. A Mn-N3 single-atom catalyst embedded in graphitic carbon nitride for efficient CO2 electroreduction. Nat Commun 2020;11:1–8. https://doi.org/10.1038/s41467-020-18143-y.
[49] Feng J, Zeng S, Jiang C, Dong H, Liu L, Zhang X. Boosting CO2 electroreduction by iodine-treated porous nitrogen-doped carbon. Chem Eng Sci X 2020;8:100084. https://doi.org/10.1016/j.cesx.2020.100084.
[50] Ju, Fengyang; Zhang, Jinjin; Lu W. Efficient electrochemical reduction of CO 2 to CO in ionic liquid/propylene carbonate electrolyte on Ag electrode 2020:1–14.
[51] Lu L, Sun X, Ma J, Yang D, Wu H, Zhang B, et al. Highly efficient electroreduction of CO2 to methanol on palladium–copper bimetallic aerogels. Angew Chem Int Ed 2018;57:14149–53. https://doi.org/10.1002/anie.201808964.
[52] Atifi A, Keane TP, Dimeglio JL, Pupillo RC, Mullins DR, Lutterman DA, et al. Insights into the composition and function of a bismuth-based catalyst for reduction of CO2 to CO. J Phys Chem C 2019;123:9087–95. https://doi.org/10.1021/acs.jpcc.9b00504.
[53] Wang H, Yang D, Yang J, Ma X, Li H, Dong W, et al. Efficient electroreduction of CO2 to CO on porous ZnO nanosheets with hydroxyl groups in ionic liquid-based electrolytes. ChemCatChem 2021;13:2570–6. https://doi.org/10.1002/cctc.202100329.
[54] Guo W, Tan X, Bi J, Xu L, Yang D, Chen C, et al. Atomic indium catalysts for switching CO2Electroreduction products from formate to CO. J Am Chem Soc 2021;143:6877–85. https://doi.org/10.1021/jacs.1c00151.
[55] Liang F, Zhang J, Hu Z, Ma C, Ni W, Zhang Y, et al. Intrinsic defect-rich graphene coupled cobalt phthalocyanine for robust electrochemical reduction of carbon dioxide. ACS Appl Mater Interfaces 2021. https://doi.org/10.1021/acsami.1c04344.
[56] Wu H, Song J, Xie C, Hu Y, Han B. Highly efficient electrochemical reduction of CO2 into formic acid over lead dioxide in an ionic liquid-catholyte mixture. Green Chem 2018;20:1765–9. https://doi.org/10.1039/c8gc00471d.
[57] Zeng M, Liu Y, Hu Y, Zhang X. High-efficient CO2 electrocatalysis over nanoporous Au film enabled by a combined pore engineering and ionic liquid-mediated approach. Chem Eng J 2021;425:131663. https://doi.org/10.1016/j.cej.2021.131663.
[58] Vedharathinam V, Qi Z, Horwood C, Bourcier B, Stadermann M, Biener J, et al. Using a 3D porous flow-through electrode geometry for high-rate electrochemical reduction of CO2 to CO in ionic liquid. ACS Catal 2019;9:10605–11. https://doi.org/10.1021/acscatal.9b03201.
[59] Hailu A, Tamijani AA, Mason SE, Shaw SK. Efficient conversion of CO2 to formate using inexpensive and easily prepared post-transition metal alloy catalysts. Energy Fuel 2020. https://doi.org/10.1021/acs.energyfuels.9b03783.
[60] Yang Y, Gao H, Feng J, Zeng S, Liu L, Liu L, et al. Aromatic ester-functionalized ionic liquid for highly efficient CO2 electrochemical reduction to oxalic acid. ChemSusChem 2020;13:4900–5. https://doi.org/10.1002/cssc.202001194.
[61] Singh MR, Clark EL, Bell AT. Effects of electrolyte, catalyst, and membrane composition and operating conditions on the performance of solar-driven electrochemical reduction of carbon dioxide. Phys Chem Chem Phys 2015;17:18924–36. https://doi.org/10.1039/c5cp03283k.
[62] Hashiba H, Weng LC, Chen Y, Sato HK, Yotsuhashi S, Xiang C, et al. Effects of electrolyte buffer capacity on surface reactant species and the reaction rate of CO2 in Electrochemical CO2 reduction. J Phys Chem C 2018;122:3719–26. https://doi.org/10.1021/acs.jpcc.7b11316.
[63] Schouten KJP, Pérez Gallent E, Koper MTM. The influence of pH on the reduction of CO and CO 2 to hydrocarbons on copper electrodes Dedicated to Professor Kingo Itaya on the occasion of his 65th birthday and in recognition of his seminal contributions to physical electrochemistry. J Electroanal Chem 2014;716:53–7. https://doi.org/10.1016/j.jelechem.2013.08.033.
[64] Xiao H, Cheng T, Goddard WA, Sundararaman R. Mechanistic explanation of the pH dependence and onset potentials for hydrocarbon products from electrochemical reduction of CO on Cu (111). J Am Chem Soc 2016;138:483–6. https://doi.org/10.1021/jacs.5b11390.
[65] Hori Y, Murata A, Takahashi R. Formation of hydrocarbons in the electrochemical reduction of carbon dioxide at a copper electrode in aqueous solution. J Chem Soc Faraday Trans 1 Phys Chem Condens Phases 1989;85:2309–26. https://doi.org/10.1039/F19898502309.
[66] Varela AS, Kroschel M, Reier T, Strasser P. Controlling the selectivity of CO2 electroreduction on copper: the effect of the electrolyte concentration and the importance of the local pH. Catal Today 2016;260:8–13. https://doi.org/10.1016/j.cattod.2015.06.009.
[67] Schouten KJP, Qin Z, Gallent EP, Koper MTM. Two pathways for the formation of ethylene in CO reduction on single-crystal copper electrodes. J Am Chem Soc 2012;134:9864–7. https://doi.org/10.1021/ja302668n.
[68] Resasco J, Chen LD, Clark E, Tsai C, Hahn C, Jaramillo TF, et al. Promoter effects of alkali metal cations on the electrochemical reduction of carbon dioxide. J Am Chem Soc 2017;139:11277–87. https://doi.org/10.1021/jacs.7b06765.
[69] Varela AS, Ju W, Reier T, Strasser P. Tuning the catalytic activity and selectivity of Cu for CO2 electroreduction in the presence of halides. ACS Catal 2016;6:2136–44. https://doi.org/10.1021/acscatal.5b02550.
[70] Gao D, Scholten F, Roldan Cuenya B. Improved CO2 electroreduction performance on plasma-activated Cu catalysts via electrolyte design: halide effect. ACS Catal 2017;7:5112–20. https://doi.org/10.1021/acscatal.7b01416.
[71] Ogura K, Ferrell JR, Cugini AV, Smotkin ES, Salazar-Villalpando MD. CO2 attraction by specifically adsorbed anions and subsequent accelerated electrochemical reduction. Electrochim Acta 2010;56:381–6. https://doi.org/10.1016/j.electacta.2010.08.065.
[72] Huang Y, Ong CW, Yeo BS. Effects of electrolyte anions on the reduction of carbon dioxide to ethylene and ethanol on copper (100) and (111) surfaces. ChemSusChem 2018;11:3299–306. https://doi.org/10.1002/cssc.201801078.
[73] Dufek EJ, Lister TE, Stone SG, McIlwain ME. Operation of a pressurized system for continuous reduction of CO 2. J Electrochem Soc 2012;159:F514–7. https://doi.org/10.1149/2.011209jes.
[74] Sonoyama N, Kirii M, Sakata T. Electrochemical reduction of CO2 at metal-porphyrin supported gas diffusion electrodes under high pressure CO2. Electrochem Commun 1999;1:213–6. https://doi.org/10.1016/S1388-2481(99)00041-7.
[75] Löwe A, Rieg C, Hierlemann T, Salas N, Kopljar D, Wagner N, et al. Influence of temperature on the performance of gas diffusion electrodes in the CO2 reduction reaction. Chemelectrochem 2019;6:4497–506. https://doi.org/10.1002/celc.201900872.
[76] Vass Endrődi B, Janáky C. Coupling electrochemical carbon dioxide conversion with value-added anode processes: an emerging paradigm. Curr Opin Electrochem 2021;25:100621. https://doi.org/10.1016/j.coelec.2020.08.003.
[77] Li R, Xiang K, Peng Z, Zou Y, Wang S. Recent advances on electrolysis for simultaneous generation of valuable chemicals at both anode and cathode. Adv Energy Mater 2021;11:1–32. https://doi.org/10.1002/aenm.202102292.
[78] Verma S, Lu S, Kenis PJA. Co-electrolysis of CO2 and glycerol as a pathway to carbon chemicals with improved technoeconomics due to low electricity consumption. Nat Energy 2019;4:466–74. https://doi.org/10.1038/s41560-019-0374-6.
[79] Guo JH, Sun WY. Integrating nickel-nitrogen doped carbon catalyzed CO2 electroreduction with chlor-alkali process for CO, Cl2 and KHCO3 production with enhanced techno-economics. Appl Catal B Environ 2020;275:119154. https://doi.org/10.1016/j.apcatb.2020.119154.
[80] Medvedeva XV, Medvedev JJ, Tatarchuk SW, Choueiri RM, Klinkova A. Sustainable at both ends: electrochemical CO2utilization paired with electrochemical treatment of nitrogenous waste. Green Chem 2020;22:4456–62. https://doi.org/10.1039/d0gc01754j.
[81] Na J, Seo B, Kim J, Lee CW, Lee H, Hwang YJ, et al. General technoeconomic analysis for electrochemical coproduction coupling carbon dioxide reduction with organic oxidation. Nat Commun 2019;10. https://doi.org/10.1038/s41467-019-12744-y.
[82] Bharath G, Hai A, Rambabu K, Kallem P, Haija MA, Banat F, et al. Fabrication of Pd/MnFe2O4 bifunctional 2-D nanosheets to enhance the yield of HCOOH from CO2 cathodic reduction paired with anodic oxidation to CH3OH. Fuel 2021;311:122619. https://doi.org/10.1016/j.fuel.2021.122619.
[83] Cao C, Ma DD, Jia J, Xu Q, Wu XT, Zhu QL. Divergent paths, same goal: a pair-electrosynthesis tactic for cost-efficient and exclusive formate production by metal–organic-framework-derived 2D electrocatalysts. Adv Mater 2021;33. https://doi.org/10.1002/adma.202008631.
[84] Wu D, Hao J, Song Z, Fu XZ, Luo JL. All roads lead to Rome: an energy-saving integrated electrocatalytic CO2 reduction system for concurrent value-added formate production. Chem Eng J 2021;412:127893. https://doi.org/10.1016/j.cej.2020.127893.
[85] Wei X, Li Y, Chen L, Shi J. Formic acid electro-synthesis by concurrent cathodic CO2 reduction and anodic CH3OH oxidation. Angew Chem Int Ed 2021;60:3148–55. https://doi.org/10.1002/anie.202012066.
[86] Tian J, Cao C, Ma D-D, Han S-G, He Y, Wu X-T, et al. Killing two birds with one stone: selective oxidation of small organic molecule as anodic reaction to boost CO 2 electrolysis. Small Struct 2021:2100134. https://doi.org/10.1002/sstr.202100134. 2100134.
[87] Li T, Cao Y, He J, Berlinguette CP. Electrolytic CO2 reduction in tandem with oxidative organic chemistry. ACS Cent Sci 2017;3:778–83. https://doi.org/10.1021/acscentsci.7b00207.
[88] Bevilacqua M, Filippi J, Lavacchi A, Marchionni A, Miller HA, Oberhauser W, et al. Energy savings in the conversion of CO2 to fuels using an electrolytic device. Energy Technol 2014;2:522–5. https://doi.org/10.1002/ente.201402014.
[89] Panglipur HS, Ivandini TA, Wibowo R, Einaga Y. Electroreduction of CO2 using copper-deposited on boron-doped diamond (BDD). In: AIP Conf. Proc., vol. 1729. American Institute of Physics Inc.; 2016. https://doi.org/10.1063/1.4946950. 020047.
[90] Bajada MA, Roy S, Warnan J, Abdiaziz K, Wagner A, Roessler MM, et al. A precious-metal-free hybrid electrolyzer for alcohol oxidation coupled to CO 2 -to-Syngas conversion. Angew Chem 2020;132:15763–71. https://doi.org/10.1002/ange.202002680.
[91] Wang G, Chen J, Li K, Huang J, Huang Y, Liu Y, et al. Cost-effective and durable electrocatalysts for Co-electrolysis of CO2 conversion and glycerol upgrading. Nano Energy 2022;92:106751. https://doi.org/10.1016/j.nanoen.2021.106751.

[92] Wang Y, Gonell S, Mathiyazhagan UR, Liu Y, Wang D, Miller AJM, et al. Simultaneous electrosynthesis of syngas and an aldehyde from CO2 and an alcohol by molecular electrocatalysis. ACS Appl Energy Mater 2019;2:97–101. https://doi.org/10.1021/acsaem.8b01616.

[93] Choi S, Balamurugan M, Lee KG, Cho KH, Park S, Seo H, et al. Mechanistic investigation of biomass oxidation using nickel oxide nanoparticles in a CO2-saturated electrolyte for paired electrolysis. J Phys Chem Lett 2020;11:2941–8. https://doi.org/10.1021/acs.jpclett.0c00425.

[94] Quan F, Zhan G, Shang H, Huang Y, Jia F, Zhang L, et al. Highly efficient electrochemical conversion of CO2 and NaCl to CO and NaClO. Green Chem 2019;21:3256–62. https://doi.org/10.1039/c9gc01099h.

[95] Kong Y, Wang L, Jiang H, Li F, Zhao T, Zhuo M, et al. Design of counter oxidation vs. CO2 electroreduction for efficient formate production on a tin cathode. J Electroanal Chem 2019;847:113264. https://doi.org/10.1016/j.jelechem.2019.113264.

[96] Lister TE, Dufek EJ. Chlor-syngas: coupling of electrochemical technologies for production of commodity chemicals. Energy Fuel 2013;27:4244–9. https://doi.org/10.1021/ef302033j.

[97] Wang Q, Wang W, Zhu C, Wu C, Yu H. A novel strategy to achieve simultaneous efficient formate production and p-nitrophenol removal in a co-electrolysis system of CO2and p-nitrophenol. J CO2 Util 2021;47:101497. https://doi.org/10.1016/j.jcou.2021.101497.

[98] Sebastián-Pascual P, Mezzavilla S, Stephens IEL, Escudero-Escribano M. Structure-sensitivity and electrolyte effects in CO2 electroreduction: from model studies to applications. ChemCatChem 2019;11:3626–45. https://doi.org/10.1002/cctc.201900552.

[99] Wang Y, Han P, Lv X, Zhang L, Zheng G. Defect and interface engineering for aqueous electrocatalytic CO 2 reduction. Joule 2018;2:2551–82. https://doi.org/10.1016/j.joule.2018.09.021.

[100] Salvatore DA, Weekes DM, He J, Dettelbach KE, Li YC, Mallouk TE, et al. Electrolysis of gaseous CO2 to CO in a flow cell with a bipolar membrane. ACS Energy Lett 2018;3:149–54. https://doi.org/10.1021/acsenergylett.7b01017.

[101] Lee W, Kim YE, Youn MH, Jeong SK, Park KT. Catholyte-free electrocatalytic CO2 reduction to formate. Angew Chem Int Ed 2018;57:6883–7. https://doi.org/10.1002/anie.201803501.

[102] Sebastián D, Palella A, Baglio V, Spadaro L, Siracusano S, Negro P, et al. CO2 reduction to alcohols in a polymer electrolyte membrane co-electrolysis cell operating at low potentials. Electrochim Acta 2017;241:28–40. https://doi.org/10.1016/j.electacta.2017.04.119.

[103] Whipple DT, Finke EC, Kenis PJA. Microfluidic reactor for the electrochemical reduction of carbon dioxide: the effect of pH. Electrochem Solid State Lett 2010;13:B109. https://doi.org/10.1149/1.3456590.

[104] Hollinger AS, Maloney RJ, Jayashree RS, Natarajan D, Markoski LJ, Kenis PJA. Nanoporous separator and low fuel concentration to minimize crossover in direct methanol laminar flow fuel cells. J Power Sources 2010;195:3523–8. https://doi.org/10.1016/j.jpowsour.2009.12.063.

[105] Lu X, Leung DYC, Wang H, Maroto-Valer MM, Xuan J. A pH-differential dual-electrolyte microfluidic electrochemical cells for CO2 utilization. Renew Energy 2016;95:277–85. https://doi.org/10.1016/j.renene.2016.04.021.

[106] Verdaguer-Casadevall A, Li CW, Johansson TP, Scott SB, McKeown JT, Kumar M, et al. Probing the active surface sites for CO reduction on oxide-derived copper electrocatalysts. J Am Chem Soc 2015;137:9808–11. https://doi.org/10.1021/jacs.5b06227.

[107] Feng X, Jiang K, Fan S, Kanan MW. A direct grain-boundary-activity correlation for CO electroreduction on Cu nanoparticles. ACS Cent Sci 2016;2:169–74. https://doi.org/10.1021/acscentsci.6b00022.

[108] Li J, Che F, Pang Y, Zou C, Howe JY, Burdyny T, et al. Copper adparticle enabled selective electrosynthesis of n-propanol. Nat Commun 2018;9:1–9. https://doi.org/10.1038/s41467-018-07032-0.

[109] Li CW, Kanan MW. CO 2 reduction at low overpotential on Cu electrodes resulting from the reduction of thick Cu 2O films. J Am Chem Soc 2012;134:7231–4. https://doi.org/10.1021/ja3010978.

[110] Baturina OA, Lu Q, Padilla MA, Xin L, Li W, Serov A, et al. CO2 electroreduction to hydrocarbons on carbon-supported Cu nanoparticles. ACS Catal 2014;4:3682–95. https://doi.org/10.1021/cs500537y.

[111] Ma M, Djanashvili K, Smith WA. Controllable hydrocarbon formation from the electrochemical reduction of CO2 over Cu nanowire arrays. Angew Chem Int Ed 2016;55:6680–4. https://doi.org/10.1002/anie.201601282.

[112] Dutta A, Rahaman M, Luedi NC, Mohos M, Broekmann P. Morphology matters: tuning the product distribution of CO2 electroreduction on oxide-derived Cu foam catalysts. ACS Catal 2016;6:3804–14. https://doi.org/10.1021/acscatal.6b00770.

[113] Yang KD, Ko WR, Lee JH, Kim SJ, Lee H, Lee MH, et al. Morphology-directed selective production of ethylene or ethane from CO 2 on a Cu mesopore electrode. Angew Chem 2017;129:814–8. https://doi.org/10.1002/ange.201610432.

[114] Zhuang TT, Pang Y, Liang ZQ, Wang Z, Li Y, Tan CS, et al. Copper nanocavities confine intermediates for efficient electrosynthesis of C3 alcohol fuels from carbon monoxide. Nat Catal 2018;1:946–51. https://doi.org/10.1038/s41929-018-0168-4.

[115] Schouten KJP, Pérez Gallent E, Koper MTM. Structure sensitivity of the electrochemical reduction of carbon monoxide on copper single crystals. ACS Catal 2013;3:1292–5. https://doi.org/10.1021/cs4002404.

[116] Loiudice A, Lobaccaro P, Kamali EA, Thao T, Huang BH, Ager JW, et al. Tailoring copper nanocrystals towards C2 products in electrochemical CO2 reduction. Angew Chem Int Ed 2016;55:5789–92. https://doi.org/10.1002/anie.201601582.

[117] Xiao H, Goddard WA, Cheng T, Liu Y. Cu metal embedded in oxidized matrix catalyst to promote CO2 activation and CO dimerization for electrochemical reduction of CO2. Proc Natl Acad Sci U S A 2017;114:6685–8. https://doi.org/10.1073/pnas.1702405114.

[118] Favaro M, Xiao H, Cheng T, Goddard WA, Crumlin EJ. Subsurface oxide plays a critical role in CO2 activation by Cu(111) surfaces to form chemisorbed CO2, the first step in reduction of CO2. Proc Natl Acad Sci U S A 2017;114:6706–11. https://doi.org/10.1073/pnas.1701405114.

[119] Bushuyev OS, De Luna P, Dinh CT, Tao L, Saur G, van de Lagemaat J, et al. What should we make with CO2 and how can we make it? Joule 2018;2:825–32. https://doi.org/10.1016/j.joule.2017.09.003.

[120] Recycling carbon dioxide in the cement industry to produce added-value additives: a step towards a CO2 circular economy. RECODE Project | H2020 | CORDIS | European Commission n.d. https://cordis.europa.eu/project/id/768583.

[121] Oxalic acid from CO2 using Eletrochemistry at demonstratioN scale. OCEAN Project | H2020 | CORDIS | European Commission 2020, https://cordis.europa.eu/project/id/767798.

[122] Integrated bio-electrochemical production of ethylene through CO2 sequestration. BIO-ELECTRO-ETHYLENE Project | FP7 | CORDIS | European Commission n.d. https://cordis.europa.eu/project/id/626959.

[123] Liu Y, Chen S, Quan X, Yu H. Efficient electrochemical reduction of carbon dioxide to acetate on nitrogen-doped nanodiamond. J Am Chem Soc 2015;137:11631–6. https://doi.org/10.1021/jacs.5b02975.

[124] Calvinho KUD, Laursen AB, Yap KMK, Goetjen TA, Hwang S, Murali N, et al. Selective CO2 reduction to C3 and C4 oxyhydrocarbons on nickel phosphides at overpotentials as low as 10 mV. Energy Environ Sci 2018;11:2550–9. https://doi.org/10.1039/c8ee00936h.

[125] Torelli DA, Francis SA, Crompton JC, Javier A, Thompson JR, Brunschwig BS, et al. Nickel-gallium-catalyzed electrochemical reduction of CO2 to highly reduced products at low overpotentials. ACS Catal 2016;6:2100–4. https://doi.org/10.1021/acscatal.5b02888.

[126] Kortlever R, Peters I, Balemans C, Kas R, Kwon Y, Mul G, et al. Palladium-gold catalyst for the electrochemical reduction of CO2 to C1-C5 hydrocarbons. Chem Commun 2016;52:10229–32. https://doi.org/10.1039/c6cc03717h.

[127] Gürü M, Bilgesü AY, Pamuk V. Production of oxalic acid from sugar beet molasses by formed nitrogen oxides. Bioresour Technol 2001;77:81–6. https://doi.org/10.1016/S0960-8524(00)00122-X.

[128] Fu C, Mahadevegowda A, Grant PS. Production of hollow and porous Fe2O3 from industrial mill scale and its potential for large-scale electrochemical energy storage applications. J Mater Chem 2016;4:2597–604. https://doi.org/10.1039/c5ta09141a.

[129] Valouma A, Verganelaki A, Tetoros I, Maravelaki-Kalaitzaki P, Gidarakos E. Magnesium oxide production from chrysotile asbestos detoxification with oxalic acid treatment. J Hazard Mater 2017;336:93–100. https://doi.org/10.1016/j.jhazmat.2017.04.019.

[130] Subramanian S, Athira KR, Anbu Kulandainathan M, Senthil Kumar S, Barik RC. New insights into the electrochemical conversion of CO2 to oxalate at stainless steel 304L cathode. J CO2 Util 2020;36:105–15. https://doi.org/10.1016/j.jcou.2019.10.011.

[131] Us 8,962,895 B2 1. Method for the production of ethylene glycol technical field. 2015.

[132] Lan J, Liao T, Zhang T, Chung LW. Reaction mechanism of Cu(I)-Mediated reductive CO2 coupling for the selective formation of oxalate: cooperative CO2 reduction to give mixed-valence Cu2(CO2•-) and nucleophilic-like attack. Inorg Chem 2017;56:6809–19. https://doi.org/10.1021/acs.inorgchem.6b03080.

[133] Zhu Y, Yu J, Brecht JK, Jiang T, Zheng X. Pre-harvest application of oxalic acid increases quality and resistance to Penicillium expansum in kiwifruit during postharvest storage. Food Chem 2016;190:537–43. https://doi.org/10.1016/j.foodchem.2015.06.001.

[134] Wang Z, Cao J, Jiang W. Changes in sugar metabolism caused by exogenous oxalic acid related to chilling tolerance of apricot fruit. Postharvest Biol Technol 2016;114:10–6. https://doi.org/10.1016/j.postharvbio.2015.11.015.

[135] Martínez-Esplá A, García-Pastor ME, Zapata PJ, Guillén F, Serrano M, Valero D, et al. Preharvest application of oxalic acid improves quality and phytochemical content of artichoke (Cynara scolymus L.) at harvest and during storage. Food Chem 2017;230:343–9. https://doi.org/10.1016/j.foodchem.2017.03.051.

[136] Zeng X, Li J, Shen B. Novel approach to recover cobalt and lithium from spent lithium-ion battery using oxalic acid. J Hazard Mater 2015;295:112–8. https://doi.org/10.1016/j.jhazmat.2015.02.064.

[137] Jin LQ, Zhao N, Liu ZQ, Liao CJ, Zheng XY, Zheng YG. Enhanced production of xylose from corncob hydrolysis with oxalic acid as catalyst. Bioproc Biosyst Eng 2018;41:57–64. https://doi.org/10.1007/s00449-017-1843-6.

[138] Treatment against honeybee varroosis based on highly effective application of oxalic acid through sublimation. BEEOXAL Project | H2020 | CORDIS | European Commission n.d. https://cordis.europa.eu/project/id/781067.

[139] Fischer J, Lehmann T, Heitz E. The production of oxalic acid from CO2 and H2O, vol. 11; 1981. https://doi.org/10.1007/BF00615179.

[140] Amatore C, Savéant J-M. Amatore and savéant 5022, vol. 103; 1981.

[141] Tomita Y, Hori Y. Electrochemical reduction of carbon dioxide at a platinum electrode in acetonitrile-water mixtures. Stud Surf Sci Catal 1998;114:581–4. https://doi.org/10.1016/s0167-2991(98)80826-4.

[142] Eneau-Innocent B, Pasquier D, Ropital F, Léger JM, Kokoh KB. Electroreduction of carbon dioxide at a lead electrode in propylene carbonate: a spectroscopic study. Appl Catal B Environ 2010;98:65–71. https://doi.org/10.1016/j.apcatb.2010.05.003.

[143] Ikeda S, Takagi T, Ito K. Selective formation of formic acid, oxalic acid, and carbon monoxide by electrochemical reduction of carbon dioxide. Bull Chem Soc Jpn 1987;60:2517–22. https://doi.org/10.1246/bcsj.60.2517.
[144] Ito K, Ikeda S, Yamauchi N, Iida T, Takagi T. Electrochemical reduction products of carbon dioxide at some metallic electrodes in nonaqueous electrolytes. Bull Chem Soc Jpn 1985;58:3027–8. https://doi.org/10.1246/bcsj.58.3027.
[145] Gennaro A, Isse AA, Severin MG, Vianello E, Bhugun I, Savéant JM. Mechanism of the electrochemical reduction of carbon dioxide at inert electrodes in media of low proton availability. J Chem Soc, Faraday Trans 1996;92:3963–8. https://doi.org/10.1039/FT9969203963.
[146] Kushi Y, Nagao H, Nishioka T, Isobe K, Tanaka K. Remarkable decrease in overpotential of oxalate formation in electrochemical CO2 reduction by a metal-sulfide cluster. J Chem Soc Chem Commun 1995;2:1223–4. https://doi.org/10.1039/C39950001223.
[147] Lv W, Zhang R, Gao P, Gong C, Lei L. Electrochemical reduction of carbon dioxide with lead cathode and zinc anode in dry acetonitrile solution. J Solid State Electrochem 2013;17:2789–94. https://doi.org/10.1007/s10008-013-2186-0.
[148] Lv WX, Zhang R, Gao PR, Gong CX, Lei LX. Electrochemical reduction of carbon dioxide on stainless steel electrode in acetonitrile. Adv Mater Res 2013;807–809:1322–5. https://dx.doi.org/10.4028/www.scientific.net/AMR.807-809.1322. Trans Tech Publications Ltd.
[149] Sun L, Ramesha GK, Kamat PV, Brennecke JF. Switching the reaction course of electrochemical CO2 reduction with ionic liquids. Langmuir 2014;30:6302–8. https://doi.org/10.1021/la5009076.
[150] Costa RS, Aranha BSR, Ghosh A, Lobo AO, da Silva ETSG, Alves DCB, et al. Production of oxalic acid by electrochemical reduction of CO2 using silver-carbon material from babassu coconut mesocarp. J Phys Chem Solid 2020;147:109678. https://doi.org/10.1016/j.jpcs.2020.109678.
[151] Senthil Kumar R, Senthil Kumar S, Anbu Kulandainathan M. Highly selective electrochemical reduction of carbon dioxide using Cu based metal organic framework as an electrocatalyst. Electrochem Commun 2012;25:70–3. https://doi.org/10.1016/j.elecom.2012.09.018.
[152] Angamuthu R, Byers P, Lutz M, Spek AL, Bouwman E. Electrocatalytic CO2 conversion to oxalate by a copper complex. Science 2010;327:313–5. https://doi.org/10.1126/science.1177981. 80.
[153] Corma A, García H, Llabrés I Xamena FX. Engineering metal organic frameworks for heterogeneous catalysis. Chem Rev 2010;110:4606–55. https://doi.org/10.1021/cr9003924.
[154] Zhou HC, Long JR, Yaghi OM. Introduction to metal-organic frameworks. Chem Rev 2012;112:673–4. https://doi.org/10.1021/cr300014x.
[155] Wang Q, Bai J, Lu Z, Pan Y, You X. Finely tuning MOFs towards high-performance post-combustion CO2 capture materials. Chem Commun 2016;52:443–52. https://doi.org/10.1039/c5cc07751f.
[156] Gandara-Loe J, Pastor-Perez L, Bobadilla LF, Odriozola JA, Reina TR. Understanding the opportunities of metal–organic frameworks (MOFs) for CO 2 capture and gas-phase CO 2 conversion processes: a comprehensive overview. React Chem Eng 2021. https://doi.org/10.1039/d1re00034a.
[157] Ghosh A, Razzino C do A, Dasgupta A, Fujisawa K, Vieira LHS, Subramanian S, et al. Structural and electrochemical properties of babassu coconut mesocarp-generated activated carbon and few-layer graphene. Carbon N Y 2019;145:175–86. https://doi.org/10.1016/j.carbon.2018.12.114.
[158] Paris AR, Bocarsly AB. High-efficiency conversion of CO 2 to oxalate in water is possible using a Cr-Ga oxide electrocatalyst. ACS Catal 2019;9:2324–33. https://doi.org/10.1021/acscatal.8b04327.
[159] Periana RA, Mironov O, Taube D, Bhalla G, Jones C. Catalytic, oxidative condensation of CH4 to CH3COOH in one step via CH activation. Science 2003;301:814–8. https://doi.org/10.1126/science.1086466. 80.
[160] Sun X, Zhu Q, Kang X, Liu H, Qian Q, Ma J, et al. Design of a Cu(I)/C-doped boron nitride electrocatalyst for efficient conversion of CO2 into acetic acid. Green Chem 2017;19:2086–91. https://doi.org/10.1039/c7gc00503b.
[161] Gadkari S, Shemfe M, Modestra JA, Mohan SV, Sadhukhan J. Understanding the interdependence of operating parameters in microbial electrosynthesis: a numerical investigation. Phys Chem Chem Phys 2019;21:10761–72. https://doi.org/10.1039/c9cp01288e.
[162] Jiang Y, Liang Q, Chu N, Hao W, Zhang L, Zhan G, et al. A slurry electrode integrated with membrane electrolysis for high-performance acetate production in microbial electrosynthesis. Sci Total Environ 2020;741:140198. https://doi.org/10.1016/j.scitotenv.2020.140198.
[163] Jourdin L, Grieger T, Monetti J, Flexer V, Freguia S, Lu Y, et al. High acetic acid production rate obtained by microbial electrosynthesis from carbon dioxide. Environ Sci Technol 2015;49:13566–74. https://doi.org/10.1021/acs.est.5b03821.
[164] Birdja YY, Koper MTM. The importance of cannizzaro-type reactions during electrocatalytic reduction of carbon dioxide. J Am Chem Soc 2017;139:2030–4. https://doi.org/10.1021/jacs.6b12008.
[165] Garza AJ, Bell AT, Head-Gordon M. Mechanism of CO2 reduction at copper surfaces: pathways to C2 products. ACS Catal 2018;8:1490–9. https://doi.org/10.1021/acscatal.7b03477.
[166] Li CW, Ciston J, Kanan MW. Electroreduction of carbon monoxide to liquid fuel on oxide-derived nanocrystalline copper. Nature 2014;508:504–7. https://doi.org/10.1038/nature13249.
[167] Grace AN, Choi SY, Vinoba M, Bhagiyalakshmi M, Chu DH, Yoon Y, et al. Electrochemical reduction of carbon dioxide at low overpotential on a polyaniline/Cu2O nanocomposite based electrode. Appl Energy 2014;120:85–94. https://doi.org/10.1016/j.apenergy.2014.01.022.
[168] Zang D, Li Q, Dai G, Zeng M, Huang Y, Wei Y. Interface engineering of Mo8/Cu heterostructures toward highly selective electrochemical reduction of carbon dioxide into acetate. Appl Catal B Environ 2021;281:119426. https://doi.org/10.1016/j.apcatb.2020.119426.
[169] Ivandini TA, Einaga Y. Electrochemical detection of selenium (IV) and (VI) at gold-modified diamond electrodes. Electrocatalysis 2013;4:367–74. https://doi.org/10.1007/s12678-013-0169-7.
[170] Hou Y, Li X, Zou X, Quan X, Chen G. Photoeletrocatalytic activity of a Cu 2O-loaded self-organized highly oriented TiO 2 nanotube array electrode for 4-chlorophenol degradation. Environ Sci Technol 2009;43:858–63. https://doi.org/10.1021/es802420u.
[171] Wang Y, Wang D, Dares CJ, Marquard SL, Sheridan MV, Meyer TJ. CO2 reduction to acetate in mixtures of ultrasmall (Cu)n,(Ag)m bimetallic nanoparticles. Proc Natl Acad Sci U S A 2017;115:278–83. https://doi.org/10.1073/pnas.1713962115.
[172] Peterson AA, Nørskov JK. Activity descriptors for CO 2 electroreduction to methane on transition-metal catalysts. J Phys Chem Lett 2012;3:251–8. https://doi.org/10.1021/jz201461p.
[173] Liu Y, Chen S, Quan X, Fan X, Zhao H, Zhao Q, et al. Nitrogen-doped nanodiamond rod array electrode with superior performance for electroreductive debromination of polybrominated diphenyl ethers. Appl Catal B Environ 2014;154–155:206–12. https://doi.org/10.1016/j.apcatb.2014.02.028.
[174] Qiao J, Liu Y, Hong F, Zhang J. A review of catalysts for the electroreduction of carbon dioxide to produce low-carbon fuels. Chem Soc Rev 2014;43:631–75. https://doi.org/10.1039/c3cs60323g.
[175] Sun X, Kang X, Zhu Q, Ma J, Yang G, Liu Z, et al. Very highly efficient reduction of CO2 to CH4 using metal-free N-doped carbon electrodes. Chem Sci 2016;7:2883–7. https://doi.org/10.1039/c5sc04158a.
[176] Liu Y, Yu H, Quan X, Chen S, Zhao H, Zhang Y. Efficient and durable hydrogen evolution electrocatalyst based on nonmetallic nitrogen doped hexagonal carbon. Sci Rep 2014;4:1–6. https://doi.org/10.1038/srep06843.
[177] Genovese C, Schuster ME, Gibson EK, Gianolio D, Posligua V, Grau-Crespo R, et al. Operando spectroscopy study of the carbon dioxide electro-reduction by iron species on nitrogen-doped carbon. Nat Commun 2018;9:1–12. https://doi.org/10.1038/s41467-018-03138-7.
[178] De R, Gonglach S, Paul S, Haas M, Sreejith SS, Gerschel P, et al. Electrocatalytic reduction of CO2 to acetic acid by a molecular manganese corrole complex. Angew Chem Int Ed 2020;59:10527–34. https://doi.org/10.1002/anie.202000601.
[179] Kumik A, Ivandini TA, Wibowo R. Modification of boron-doped diamond with gold-palladium nanoparticles for CO2 electroreduction. In: IOP Conf. Ser. Mater. Sci. Eng., vol. 763. Institute of Physics Publishing; 2020. https://doi.org/10.1088/1757-899X/763/1/012001. 012001.
[180] Li C, Zha B, Li J. A SiW11Mn-assisted indium electrocatalyst for carbon dioxide reduction into formate and acetate. J CO2 Util 2020;38:299–305. https://doi.org/10.1016/j.jcou.2020.02.008.
[181] Yang H, Zhang C, Gao P, Wang H, Li X, Zhong L, et al. A review of the catalytic hydrogenation of carbon dioxide into value-added hydrocarbons. Catal Sci Technol 2017;7:4580–98. https://doi.org/10.1039/c7cy01403a.
[182] Guo L, Sun J, Ge Q, Tsubaki N. Recent advances in direct catalytic hydrogenation of carbon dioxide to valuable C2+ hydrocarbons. J Mater Chem 2018;6:23244–62. https://doi.org/10.1039/c8ta05377d.
[183] Zhou W, Cheng K, Kang J, Zhou C, Subramanian V, Zhang Q, et al. New horizon in C1 chemistry: breaking the selectivity limitation in transformation of syngas and hydrogenation of CO2 into hydrocarbon chemicals and fuels. Chem Soc Rev 2019;48:3193–228. https://doi.org/10.1039/c8cs00502h.
[184] Maffia GJ, Gaffney AM, Mason OM. Techno-economic analysis of oxidative dehydrogenation options. Top Catal 2016;59:1573–9. https://doi.org/10.1007/s11244-016-0677-9.
[185] Gaffney AM, Mason OM. Ethylene production via oxidative dehydrogenation of ethane using M1 catalyst. Catal Today 2017;285:159–65. https://doi.org/10.1016/j.cattod.2017.01.020.
[186] De Luna P, Hahn C, Higgins D, Jaffer SA, Jaramillo TF, Sargent EH. What would it take for renewably powered electrosynthesis to displace petrochemical processes?. 80 Science 2019:364. https://doi.org/10.1126/science.aav3506. eaav3506.
[187] Li F, Thevenon A, Rosas-Hernández A, Wang Z, Li Y, Gabardo CM, et al. Molecular tuning of CO2-to-ethylene conversion. Nature 2020;577:509–13. https://doi.org/10.1038/s41586-019-1782-2.
[188] Kuhl KP, Cave ER, Abram DN, Jaramillo TF. New insights into the electrochemical reduction of carbon dioxide on metallic copper surfaces. Energy Environ Sci 2012;5:7050–9. https://doi.org/10.1039/c2ee21234j.
[189] Hori Y, Wakebe H, Tsukamoto T, Koga O. Electrocatalytic process of CO selectivity in electrochemical reduction of CO2 at metal electrodes in aqueous media. Electrochim Acta 1994;39:1833–9. https://doi.org/10.1016/0013-4686(94)85172-7.
[190] Calle-Vallejo F, Koper MTM. Theoretical considerations on the electroreduction of CO to C2 Species on Cu(100) electrodes. Angew Chem Int Ed 2013;52:7282–5. https://doi.org/10.1002/anie.201301470.
[191] Li Y, Sun Q. Recent advances in breaking scaling relations for effective electrochemical conversion of CO2. Adv Energy Mater 2016;6:1600463. https://doi.org/10.1002/aenm.201600463.
[192] Montoya JH, Shi C, Chan K, Nørskov JK. Theoretical insights into a CO dimerization mechanism in CO2 electroreduction. J Phys Chem Lett 2015;6:2032–7. https://doi.org/10.1021/acs.jpclett.5b00722.

[193] Friebe P, Bogdanoff P, Alonso-Vante N, Tributsch H. A real-time mass spectroscopy study of the (electro)chemical factors affecting CO2 reduction at copper. J Catal 1997;168:374–85. https://doi.org/10.1006/jcat.1997.1606.
[194] Xie C, Niu Z, Kim D, Li M, Yang P. Surface and interface control in nanoparticle catalysis. Chem Rev 2020;120:1184–249. https://doi.org/10.1021/acs.chemrev.9b00220.
[195] Goodpaster JD, Bell AT, Head-Gordon M. Identification of possible pathways for C-C bond formation during electrochemical reduction of CO2: new theoretical insights from an improved electrochemical model. J Phys Chem Lett 2016;7:1471–7. https://doi.org/10.1021/acs.jpclett.6b00358.
[196] Jiang K, Sandberg RB, Akey AJ, Liu X, Bell DC, Nørskov JK, et al. Metal ion cycling of Cu foil for selective C-C coupling in electrochemical CO2 reduction. Nat Catal 2018;1:111–9. https://doi.org/10.1038/s41929-017-0009-x.
[197] Mistry H, Varela AS, Bonifacio CS, Zegkinoglou I, Sinev I, Choi YW, et al. Highly selective plasma-activated copper catalysts for carbon dioxide reduction to ethylene. Nat Commun 2016;7:12123. https://doi.org/10.1038/ncomms12123.
[198] Zhou Y, Che F, Liu M, Zou C, Liang Z, De Luna P, et al. Dopant-induced electron localization drives CO2 reduction to C2 hydrocarbons. Nat Chem 2018;10:974–80. https://doi.org/10.1038/s41557-018-0092-x.
[199] Roberts FS, Kuhl KP, Nilsson A. High selectivity for ethylene from carbon dioxide reduction over copper nanocube electrocatalysts. Angew Chem 2015;127:5268–71. https://doi.org/10.1002/ange.201412214.
[200] Zhang B, Zhang J, Hua M, Wan Q, Su Z, Tan X, et al. Highly electrocatalytic ethylene production from CO2on nanodefective Cu nanosheets. J Am Chem Soc 2020;142:13606–13. https://doi.org/10.1021/jacs.0c06420.
[201] Ren D, Deng Y, Handoko AD, Chen CS, Malkhandi S, Yeo BS. Selective electrochemical reduction of carbon dioxide to ethylene and ethanol on copper(I) oxide catalysts. ACS Catal 2015;5:2814–21. https://doi.org/10.1021/cs502128q.
[202] Lee SY, Jung H, Kim NK, Oh HS, Min BK, Hwang YJ. Mixed copper states in anodized Cu electrocatalyst for stable and selective ethylene production from CO 2 reduction. J Am Chem Soc 2018;140:8681–9. https://doi.org/10.1021/jacs.8b02173.
[203] Vasileff A, Xu C, Jiao Y, Zheng Y, Qiao SZ. Surface and interface engineering in copper-based bimetallic materials for selective CO2 electroreduction. Inside Chem 2018;4:1809–31. https://doi.org/10.1016/j.chempr.2018.05.001.
[204] Zheng T, Jiang K, Wang H. Recent advances in electrochemical CO2-to-CO conversion on heterogeneous catalysts. Adv Mater 2018;30:1802066. https://doi.org/10.1002/adma.201802066.
[205] Kim C, Dionigi F, Beermann V, Wang X, Möller T, Strasser P. Alloy nanocatalysts for the electrochemical oxygen reduction (ORR) and the direct electrochemical carbon dioxide reduction reaction (CO2RR). Adv Mater 2019;31:1805617. https://doi.org/10.1002/adma.201805617.
[206] Chang Z, Huo S, Zhang W, Fang J, Wang H. The tunable and highly selective reduction products on Ag@Cu bimetallic catalysts toward CO2 electrochemical reduction reaction. J Phys Chem C 2017;121:11368–79. https://doi.org/10.1021/acs.jpcc.7b01586.
[207] Hoang TTH, Verma S, Ma S, Fister TT, Timoshenko J, Frenkel AI, et al. Nanoporous copper-silver alloys by additive-controlled electrodeposition for the selective electroreduction of CO2 to ethylene and ethanol. J Am Chem Soc 2018;140:5791–7. https://doi.org/10.1021/jacs.8b01868.
[208] Ma S, Sadakiyo M, Heim M, Luo R, Haasch RT, Gold JI, et al. Electroreduction of carbon dioxide to hydrocarbons using bimetallic Cu-Pd catalysts with different mixing patterns. J Am Chem Soc 2017;139:47–50. https://doi.org/10.1021/jacs.6b10740.
[209] Andersen M, Medford AJ, Nørskov JK, Reuter K. Scaling-relation-based analysis of bifunctional catalysis: the case for homogeneous bimetallic alloys. ACS Catal 2017;7:3960–7. https://doi.org/10.1021/acscatal.7b00482.
[210] Li X, Zhu Q-L. MOF-based materials for photo- and electrocatalytic CO2 reduction. Energy 2020;2:100033. https://doi.org/10.1016/j.enchem.2020.100033.
[211] Schneider J, Jia H, Muckerman JT, Fujita E. Thermodynamics and kinetics of CO2, CO, and H+ binding to the metal centre of CO2 reduction catalysts. Chem Soc Rev 2012;41:2036–51. https://doi.org/10.1039/c1cs15278e.
[212] Han N, Ding P, He L, Li Y, Li Y. Promises of main group metal–based nanostructured materials for electrochemical CO2 reduction to formate. Adv Energy Mater 2020;10:1902338. https://doi.org/10.1002/aenm.201902338.
[213] Nam DH, Bushuyev OS, Li J, De Luna P, Seifitokaldani A, Dinh CT, et al. Metal-organic frameworks mediate Cu coordination for selective CO2 electroreduction. J Am Chem Soc 2018;140:11378–86. https://doi.org/10.1021/jacs.8b06407.
[214] Chen X, Ma DD, Chen B, Zhang K, Zou R, Wu XT, et al. Metal–organic framework-derived mesoporous carbon nanoframes embedded with atomically dispersed Fe–Nx active sites for efficient bifunctional oxygen and carbon dioxide electroreduction. Appl Catal B Environ 2020;267:118720. https://doi.org/10.1016/j.apcatb.2020.118720.
[215] Ren W, Tan X, Yang W, Jia C, Xu S, Wang K, et al. Isolated diatomic Ni-Fe metal–nitrogen sites for synergistic electroreduction of CO2. Angew Chem Int Ed 2019;58:6972–6. https://doi.org/10.1002/anie.201901575.
[216] Cheng YS, Chu XP, Ling M, Li N, Wu KL, Wu FH, et al. An MOF-derived copper@nitrogen-doped carbon composite: the synergistic effects of N-types and copper on selective CO2 electroreduction. Catal Sci Technol 2019;9:5668–75. https://doi.org/10.1039/c9cy01131e.
[217] Yang F, Chen A, Deng PL, Zhou Y, Shahid Z, Liu H, et al. Highly efficient electroconversion of carbon dioxide into hydrocarbons by cathodized copper-organic frameworks. Chem Sci 2019;10:7975–81. https://doi.org/10.1039/c9sc02605c.
[218] Zheng Y, Cheng P, Xu J, Han J, Wang D, Hao C, et al. MOF-derived nitrogen-doped nanoporous carbon for electroreduction of CO2 to CO: the calcining temperature effect and the mechanism. Nanoscale 2019;11:4911–7. https://doi.org/10.1039/c8nr10236h.
[219] Guan A, Chen Z, Quan Y, Peng C, Wang Z, Sham TK, et al. Boosting CO2 electroreduction to CH4 via tuning neighboring single-copper sites. ACS Energy Lett 2020;5:1044–53. https://doi.org/10.1021/acsenergylett.0c00018.
[220] Zhu Q, Sun X, Yang D, Ma J, Kang X, Zheng L, et al. Carbon dioxide electroreduction to C2 products over copper-cuprous oxide derived from electrosynthesized copper complex. Nat Commun 2019;10:3851. https://doi.org/10.1038/s41467-019-11599-7.
[221] Mizik T, Nagy L, Gabnai Z, Bai A. The major driving forces of the EU and US ethanol markets with special attention paid to the COVID-19 pandemic. Energies 2020;13:5614. https://doi.org/10.3390/en13215614.
[222] Renewable Fuels Association. Focus forward: 2020 ethanol industry outlook. DC: Washingto; 2020.
[223] Niphadkar S, Bagade P, Ahmed S. Bioethanol production: insight into past, present and future perspectives. Biofuels 2018;9:229–38. https://doi.org/10.1080/17597269.2017.1334338.
[224] Yuan J, Yang MP, Zhi WY, Wang H, Wang H, Lu JX. Efficient electrochemical reduction of CO2 to ethanol on Cu nanoparticles decorated on N-doped graphene oxide catalysts. J CO2 Util 2019;33:452–60. https://doi.org/10.1016/j.jcou.2019.07.014.
[225] Lee S, Park G, Lee J. Importance of Ag-Cu biphasic boundaries for selective electrochemical reduction of CO2 to ethanol. ACS Catal 2017;7:8594–604. https://doi.org/10.1021/acscatal.7b02822.
[226] Tang W, Peterson AA, Varela AS, Jovanov ZP, Bech L, Durand WJ, et al. The importance of surface morphology in controlling the selectivity of polycrystalline copper for CO2 electroreduction. Phys Chem Chem Phys 2012;14:76–81. https://doi.org/10.1039/c1cp22700a.
[227] Ren D, Wong NT, Handoko AD, Huang Y, Yeo BS. Mechanistic insights into the enhanced activity and stability of agglomerated Cu nanocrystals for the electrochemical reduction of carbon dioxide to n-propanol. J Phys Chem Lett 2016;7:20–4. https://doi.org/10.1021/acs.jpclett.5b02554.
[228] Le M, Ren M, Zhang Z, Sprunger PT, Kurtz RL, Flake JC. Electrochemical reduction of CO2 to CH3OH at copper oxide surfaces. J Electrochem Soc 2011;158:E45. https://doi.org/10.1149/1.3561636.
[229] Li Q, Fu J, Zhu W, Chen Z, Shen B, Wu L, et al. Tuning Sn-catalysis for electrochemical reduction of CO2 to CO via the core/shell Cu/SnO2 structure. J Am Chem Soc 2017;139:4290–3. https://doi.org/10.1021/jacs.7b00261.
[230] Duan YX, Meng FL, Liu KH, Yi SS, Li SJ, Yan JM, et al. Amorphizing of Cu nanoparticles toward highly efficient and robust electrocatalyst for CO2 reduction to liquid fuels with high faradaic efficiencies. Adv Mater 2018;30:1706194. https://doi.org/10.1002/adma.201706194.
[231] Singh MR, Clark EL, Bell AT. Thermodynamic and achievable efficiencies for solar-driven electrochemical reduction of carbon dioxide to transportation fuels. Proc Natl Acad Sci U S A 2015;112. https://doi.org/10.1073/pnas.1519212112. E6111–8.
[232] Hori Y, Takahashi I, Koga O, Hoshi N. Electrochemical reduction of carbon dioxide at various series of copper single crystal electrodes. J Mol Catal Chem 2003;199:39–47. https://doi.org/10.1016/S1381-1169(03)00016-5.
[233] Eilert A, Cavalca F, Roberts FS, Osterwalder J, Liu C, Favaro M, et al. Subsurface oxygen in oxide-derived copper electrocatalysts for carbon dioxide reduction. J Phys Chem Lett 2017;8:285–90. https://doi.org/10.1021/acs.jpclett.6b02273.
[234] Handoko AD, Ong CW, Huang Y, Lee ZG, Lin L, Panetti GB, et al. Mechanistic insights into the selective electroreduction of carbon dioxide to ethylene on Cu2O-derived copper catalysts. J Phys Chem C 2016;120. https://doi.org/10.1021/acs.jpcc.6b07128. 20058–67.
[235] Daiyan R, Saputera WH, Zhang Q, Lovell E, Lim S, Ng YH, et al. 3D heterostructured copper electrode for conversion of carbon dioxide to alcohols at low overpotentials. Adv Sustain Syst 2019;3:1800064. https://doi.org/10.1002/adsu.201800064.
[236] Shen S, Peng X, Song L, Qiu Y, Li C, Zhuo L, et al. AuCu alloy nanoparticle embedded Cu submicrocone arrays for selective conversion of CO2 to ethanol. Small 2019;15:1902229. https://doi.org/10.1002/smll.201902229.
[237] Albo J, Perfecto-Irigaray M, Beobide G, Irabien A. Cu/Bi metal-organic framework-based systems for an enhanced electrochemical transformation of CO2 to alcohols. J CO2 Util 2019;33:157–65. https://doi.org/10.1016/j.jcou.2019.05.025.
[238] Albo J, Vallejo D, Beobide G, Castillo O, Castaño P, Irabien A. Copper-based metal–organic porous materials for CO2 electrocatalytic reduction to alcohols. ChemSusChem 2017;10:1100–9. https://doi.org/10.1002/cssc.201600693.
[239] Zhao K, Liu Y, Quan X, Chen S, Yu H. CO2 electroreduction at low overpotential on oxide-derived Cu/carbons fabricated from metal organic framework. ACS Appl Mater Interfaces 2017;9:5302–11. https://doi.org/10.1021/acsami.6b15402.
[240] Klabunde J, Bischoff C, Papa AJ. Propanols. Ullmann's encycl. Ind. Chem. Weinheim, Germany: Wiley-VCH Verlag GmbH & Co. KGaA; 2018. p. 1–14. https://doi.org/10.1002/14356007.a22_173.pub3.
[241] Atsumi S, Hanai T, Liao JC. Non-fermentative pathways for synthesis of branched-chain higher alcohols as biofuels. Nature 2008;451:86–9. https://doi.org/10.1038/nature06450.
[242] Hori Y, Takahashi R, Yoshinami Y, Murata A. Electrochemical reduction of CO at a copper electrode. J Phys Chem B 1997;101:7075–81. https://doi.org/10.1021/jp970284i.

[243] Jouny M, Luc W, Jiao F. General techno-economic analysis of CO2 electrolysis systems. Ind Eng Chem Res 2018;57:2165–77. https://doi.org/10.1021/acs.iecr.7b03514.
[244] Kibria MG, Edwards JP, Gabardo CM, Dinh CT, Seifitokaldani A, Sinton D, et al. Electrochemical CO2 reduction into chemical feedstocks: from mechanistic electrocatalysis models to system design. Adv Mater 2019;31:1807166. https://doi.org/10.1002/adma.201807166.
[245] Raizada T. US acetic acid demand soft in the Americas. ICIS News; 2016. https://www.icis.com/explore/resources/news/2016/09/02/10031371/us-acetic-acid-demand-soft-in-the-americas/.
[246] China petroleum & chemical industry association: petrochemical price: inorganic chemical material. 2020. https://www.ceicdata.com/en/china/china-petroleum–chemical-industry-association-petrochemical-price-organic-chemical-material.
[247] Phosphoric acid price market analysis - echemi. Echemi; 2020. https://www.echemi.com/productsInformation/temppid160705011349-oxalic-acid.html.
[248] Global acetic acid market to reach 11.85 million tons by 2026. 2020. significant growth during 2016-2020, https://www.expertmarketresearch.com/pressrelease/global-acetic-acid-market#:~:text=According to a new report.
[249] Global oxalic acid size expected to grow at 4.0% CAGR by 2025 n.d. https://www.adroitmarketresearch.com/press-release/global-oxalic-acid-market-size-and-forecast-2012-2025.
[250] Global calcium carbonate market size report. 2020-2027 2020:1–118, https://www.grandviewresearch.com/industry-analysis/calcium-carbonate-market.
[251] Sisler J, Khan S, Ip AH, Schreiber MW, Jaffer SA, Bobicki ER, et al. Ethylene electrosynthesis: a comparative techno-economic analysis of alkaline vs membrane electrode assembly vs CO2-CO-C2H4Tandems. ACS Energy Lett 2021:997–1002. https://doi.org/10.1021/acsenergylett.0c02633.